STUDY OF THREADING OPERATIONS IN AUSTEMPERED DUCTILE IRON

by

Matthew Candelas, B.S.T

A thesis submitted to the Graduate Council of
Texas State University in partial fulfillment
of the requirements for the degree of
Master of Science
with a Major in Engineering Management
December 2022

Committee Members:

Luis Trueba, Chair

Farhad Ameri

Robert Habingreither

COPYRIGHT

by

Matthew Candelas

2022

FAIR USE AND AUTHOR'S PERMISSION STATEMENT

Fair Use

This work is protected by the Copyright Laws of the United States (Public Law 94-553, section 107). Consistent with fair use as defined in the Copyright Laws, brief quotations from this material are allowed with proper acknowledgement. Use of this material for financial gain without the author's express written permission is not allowed.

Duplication Permission

As the copyright holder of this work I, Matthew Candelas, authorize duplication of this work, in whole or in part, for educational or scholarly purposes only.

DEDICATION

Dedicated to my family and friends.

ACKNOWLEDGEMENTS

Completion of this study would not have been possible without the help of several individuals who donated their time and expertise to me. I would like to thank Chris Heczko, Tim Heagney, and Tyler Towns for their help in acquiring the ductile iron used in my research. I would also like to thank Dura-Bar for their generous donation.

I would like to thank Jeremy Lipshaw, Tony Geyman, Cody Wilson, Connor Montgomery, and everyone at Applied Process that helped with the austempering of my iron samples. Thank you to Steve Metz for the time spent analyzing the images I sent and for the information you provided about ADI grain structures.

Thank you to Matthew Hernandez at Harvey Tool for researching and providing thread milling feeds and speeds.

Thank you to David Allen at Kistler for being so responsive and patient, and for walking me through the operation of the dynamometer.

Thank you to Jacob Armitage and the TXST ARSC for their support on the XRD

A special thanks to Scott Lammers and the Ductile Iron Society for putting me in contact with Jeremy, for their support of my research, and for providing boxes of literature.

Thank you to Collin Payne, Corbin Hanzel, Marcus Ickes, and Marcus Goss for providing access to the tools and equipment I needed to conduct my research.

Thank you to Juan Gomez for all the help with outlines, suggestions, advice, proofreading, and for the collective gallons of iced coffee.

Thank you to Dr. Ameri for always being so supportive of everything I wanted to do, for helping me with the admission process, for advising me in all my coursework, and for agreeing to be a member of my committee.

Thank you to Dr. Habingreither for always having a story or a joke on tap, for pushing me to go to grad school in the first place, and for agreeing to sit on my committee when you would rather be enjoying retirement on a mountain in New Mexico.

Thank you to Dr. Trueba, for taking me on as a researcher, for supporting me through all of my indecisiveness and for being an endless supply of advice and knowledge.

I would like to thank my friends for always asking if I was ever going to graduate and not giving me too hard of a time when I shrugged and said, “Next semester, for sure.”

Thank you to my family for their patience and for always supporting me no matter what I decide to do. For being interested in my research just because it’s a part of my life. Thank you to the Nemecs, it should go without saying that I was of course addressing y’all too when I said family. Thank you all for treating me like I’m another son.

Finally, thank you to Julie, the most important person in my life, my best friend. For growing up with me, living life with me, and for always pushing me to move forward when I’m ready to give up. I love you, forever & always.

TABLE OF CONTENTS

Page

ACKNOWLEDGEMENTS v

LIST OF TABLES ix

LIST OF FIGURES x

LIST OF ABBREVIATIONS xii

ABSTRACT xiii

CHAPTER

1. INTRODUCTION 1

    1.1 Motivation 1
    1.2 Problem Statement 5
    1.3 Objective Statement 6
        1.3.1 Primary Objective 6
        1.3.2 Secondary Objectives 6
    1.4 Outline of the Thesis 6
    1.5 Review of Relevant Literature 6
    1.6 Discussion of Threading Methods 10
        1.6.1 Cut Tapping 10
        1.6.2 Form Tapping 11
        1.6.3 Thread Milling 13
    1.7 Discussion of Feeds and Speeds 15
        1.7.1 Feed 15
        1.7.2 Speed 15

2. MATERIALS AND METHODS 17

    2.1 Ductile Iron 17
        2.1.1 Material Acquisition 17
        2.1.2 Properties 18
        2.1.3 Sample Preparation 19
    2.2 Cutting Tools 23
    2.3 CNC Mill 27

2.4 Dynamometer 27
2.5 Experimental Procedures 30
2.6 Design of Experiment 34
2.7 Characterization 35

3. RESULTS AND DISCUSSION 37

3.1 Observations 37
3.1.1 Dimensional Changes in Samples 37
3.1.2 Tool Wear 38
3.1.3 Catastrophic Tool Failure 38
3.1.4 Dynamometer Data 44
3.1.5 Chip Morphology 45
3.1.6 Thread Profile and Surface Finish 49
3.1.7 Metallography After Machining 50
3.2 Discussion 53

4. CONCLUSIONS 57

4.1 Future Research 58
4.2 Post Experimental Thoughts 58

APPENDIX SECTION 59

REFERENCES 67

LIST OF TABLES

Table **Page**

2.1: 65-45-12 Iron Matrix Composition and Nodule Count 18

2.2: Chemical Composition of Iron Bar 18

2.3: Tensile Properties of 65-45-12 Iron Sample 19

2.4: As-Cast Iron Bar Hardness Certification 19

2.5: Average Hardness of Iron Samples 22

2.6: Tools Utilized in the Study 26

2.7: Feeds and Speeds of Tools on ADI 27

2.8: Operation Feeds, Speeds, and Frequencies 30

2.9: Design of Experiment 35

3.1: Observed Iron Growth after Austempering 37

3.2: Torque Values Observed in Rigid Tapping Operations 45

3.3: Sample Surface Finish 50

LIST OF FIGURES

Figure **Page**

1.1: Grain structure of material matrixes after threading 14

2.1: Points of measurement on test specimens 21

2.2: Specimen block dimensions and threaded hole pattern 21

2.3: Heat tinted microstructure of sample 4B 23

2.4: Kistler Type 9170-A rotating dynamometer with carbide insert drill 29

2.5: Probing a specimen to establish the WCS for the CNC operation 32

2.6: Mastercam programming environment with drilling/tapping operation movements displayed 33

2.7: Mastercam programming environment with thread milling operation movements displayed 33

2.8: Experimental setup for drilling operations 34

3.1: Light microscopy image of cut tap flute number 4 wear after 28 holes 39

3.2: Cut tap flute wear after 28 holes. Crater wear is visible on the tool rake face 40

3.3: Topographical image of cut tap flute 4 after 28 holes 40

3.4: Lobe wear on the form tap insert after 28 holes 41

3.5: Form tap lobe wear after 28 holes 41

3.6: Form tap lobe wear after 28 holes 42

3.7: An unused carbide drill insert 42

3.8: Drill insert rake face after 56 holes in ADI 43

3.9: Drill insert flank after 56 holes in ADI 43

3.10: Typical short, segmented chip produced when drilling ADI 46

3.11: Topographical image of the short, segmented ADI chip 46

3.12: Segmented chips from drilling flipped 47

3.13: Medium length continuous ADI chip from drilling 48

3.14: Long continuous ADI drilling chip curling along a constantly tightening spiral 48

3.15: Long continuous chip from drilling as-cast 65-45-12 ductile iron 48

3.16: Sample 1A formed (50%) thread valley heat tinted microstructure 51

3.17: Sample 2A cut thread valley heat tinted microstructure 52

3.18: Sample 4B Formed (75%) thread valley heat tinted microstructure 53

LIST OF ABBREVIATIONS

Abbreviation	Description
ADI	Austempered Ductile Iron
SIT	Stress Induced Transformation
CNC	Computer Numerical Control
SFM	Surface Feet per Minute
FPT	Feed Per Tooth
HSS	High Speed Steel
MQL	Minimum Quantity Lubrication

ABSTRACT

The focus of this research was to compare three different methods of threading holes into grade 1 ADI and to determine the viability of plastically deforming threads (thread forming) into ADI rather than cutting the material. Identical test specimens were drilled with carbide tipped drills and threaded by cut taps, forming taps, and thread mills. Data used to evaluate the threading methods included cutting force data, surface profilometry, and metallographic analysis. Thread forming was successful and, under the appropriate conditions, can surpass the performance of a cut tap. Threads that were formed had a greater concentration of martensite within the matrix at the threads than those that were cut. Threads formed at 50% thread formation consumed an average of 78% more energy than threads that were cut with a tap. Increasing the thread formation to 75% from 50% in forming operations increased the average energy consumption by 260%. Thread milling was successful but took significantly longer than the other two methods. Threads produced by cutting having an average surface finish Ra that is 27.7% lower (finer) than formed threads.

Keywords: Machinability, Austempered, ADI, Threading, Forming

1. INTRODUCTION

1.1 Motivation

Austempered Ductile Iron (ADI) is a material with properties that make it an attractive option for a variety of engineering applications. There are five grades of ADI that feature a wide range of mechanical properties. The ADI family is used across a variety of applications including gear trains, suspension components, and ground engagement tools. It is commonly used in rolling or abrasive applications for its impressive toughness, wear resistance, and fatigue strength. The strength-to-weight ratio of ADI is superior to aluminum alloys and meets or exceeds most steel alloys. A moderate cost makes ADI a nearly perfect candidate for many applications, were it not for its reputation as a material that is difficult to machine [1], [2].

ADI is produced by subjecting a ductile cast iron component to a two-step heat treatment called austempering. During austempering the iron is austenitized long enough for carbon to saturate the austenite within the matrix and then it is isothermally quenched and held above the martensite start temperature until the matrix has fully transformed into ausferrite. This heat treatment results in a material that remains ductile but is in a class of metals that undergo stress induced transformation (SIT). During SIT the crystalline structure of the material is placed under sufficient mechanical stress and high-carbon metastable austenite within the microstructure is transformed into martensite [3]. Martensite is a harder and tougher allotrope of iron and carbon than austenite and this significantly increases the aggregate hardness and toughness of the bulk material [4].

ADI has been used in several automotive applications; however, it is typically limited to cast components that are near net shape and do not require tight tolerances on

machined features [1]. Before austempering, ductile iron is a free machining material and does not require any special processes or accommodations [5]. The most common manufacturing technique is to take as-cast ductile iron parts and machine any necessary features prior to being heat treated [1]. The primary issue with this approach is the dimensional growth of the workpiece during heat treatment. Scale and oxides also form on the part surface during austempering so applications with surface finish requirements may be incompatible with this manufacturing approach as well. If the design calls for tolerances that are reasonably loose the part growth can be predicted and accounted for prior to austempering. However, if critical features are precisely located on the part and the iron is then austempered, accuracy of the features cannot be guaranteed to within a few ten-thousandths of an inch. The magnitude of potential error due to part growth scales with the size of the casting [6].

Many components manufactured today require repeatable, tight tolerances so a process that alters the position and shape of critical features after they have been placed on the part is unacceptable in many situations. Therefore, the only way to ensure the accurate placement of machined features onto an ADI part is to machine the parts after they have been austempered.

Another common approach when dealing with ADI is to rough machine the as-cast component, austemper, and then finish machine in the austempered state [1]. This approach presents logistical challenges as it must be setup for rough machining, shipped to heat treatment, returned, and setup again for finish machining. The increased number of steps increases lead times and cost of production, reducing or eliminating the savings that ADI initially had when compared to more common material alternatives.

Machining after heat treatment poses a problem to manufacturers because ADI's machinability is much lower than as cast ductile iron. The same mechanical properties that make ADI an attractive option-like its wear resistance and toughness-also act as factors that abrade and wear out cutting tools. The SIT phenomenon results in the material becoming significantly more difficult to deform immediately before being acted on by the leading edge of the tool in a machining operation [7].

Machining technology in the 1970's was primarily based around high-speed steel (HSS) cutting tools and manual machining centers. Over the last 50 years, cutting tools have evolved considerably with the advent of tool materials with superior hardness, abrasion resistance, and higher temperature tolerance. Tungsten carbide, being one of those materials, has largely replaced HSS tooling in many manufacturing operations due to its ability to last longer and remove material faster [8]. That is not to say HSS no longer has a place in subtractive manufacturing. HSS is tougher than carbide, making it a good choice for operations where the tool will be subject to shock, chatter, or deflection. The benefits of carbide can only be realized if machining setup conditions are ideal; unfortunately that is not always a possibility.

Milling and turning centers have also advanced from manual and early punch tape numerical controlled machines to modern computer numerical controlled (CNC) machines. Greater machine precision enables the manufacturer to engage the workpiece at an optimal feed rate and radial stepover for a given cutter which optimizes the material removal rate (MRR) while also maximizing tool life and part surface finish. For threading operations these machines also offer the programmer the capability of synchronizing axis movement with spindle rotation to tap holes without the use of clutched tapping heads,

torque limiting collets, and tension-compression toolholders [9]. CNC milling machines and lathes equipped with live tooling are also capable of helically interpolating a thread form using a rotating cutting tool [10].

With the advances in subtractive manufacturing over the last two decades the issue of ADI machinability is no longer due to tooling limitations and machine capabilities but rather a lack of documented parameters and processes that leverage the capabilities of the latest technology. ADI is a phenomenal and cost-effective material that is often overlooked due to a reputation it developed because of the limitations of outdated technology and a misunderstanding of how it should be processed. The mystique surrounding the machining of ADI continues to be perpetuated by a lack of recommendations for processes and starting parameters. A machinist who had not worked with ADI would likely refer to a feeds and speeds database or reference literature, only to be disappointed by the lack of information. "The Machinery's Handbook" is the self-proclaimed "Bible of the Mechanical Industries" and many machinists' go-to source for process recommendations, however as of the 31st edition it contains no information on the machining of ADI. If a private manufacturing operation has invested resources into developing a database of preferred processes and parameters, they would consider them to be a competitive advantage and withhold them from the public domain.

Recent studies on ADI machinability have just begun to develop general milling and turning recommendations. The authors of these papers provide the reader with the method and parameters they used and the degree of success they observed when milling, drilling, and turning ADI workpieces. Current research regarding threading is limited and focuses on wear observed on cut taps. No research has been published evaluating the

viability of alternative threading methods at a machinist's disposal. This comparison of alternative threading methods and process parameters for ADI within the public domain will provide clarity on what options a machinist working with ADI can choose from. This would ultimately empower manufacturers across many industries to feel more comfortable in substituting ADI for more expensive alloys with inferior properties. Such substitutions could improve product reliability while also reducing part weight, complexity, and production time resulting in millions of dollars saved across industries that chose to implement these changes.

If ADI is to be fully embraced by manufacturers, the list of appropriate processes for all types of operations needs to be complete. This study on threading operations helps to fill the void in manufacturing's understanding of threading ADI workpieces.

1.2 Problem Statement

ADI is tougher and more abrasive on cutting tools than traditional free machining materials. It carries a reputation of poor machinability, and there are no publicly available recommendations for processes that have been proven to produce threaded holes, which makes the material less appealing to a product designer. ADI is a tough material that is known to wear cutting edges and break tools. Threading methods that can produce acceptable threads must be determined. The following questions were investigated:

- Are cut tapping, thread milling, and form tapping viable options for producing threaded holes in an ADI workpiece?
- How does productivity of the different methods compare?
- How do the resulting threads of the different methods compare?

1.3 Objective Statement

1.3.1 Primary Objective

Determine the viability of thread forming and thread milling when using a CNC mill to thread holes into an ADI workpiece.

1.3.2 Secondary Objectives

- Compare the process properties of the available methods.
- Compare the thread properties of the available methods.

The following properties were used to evaluate the threading methods used in this study:

- Cutting force measurements.
- Metallographic analysis
- Thread surface finish

1.4 Outline of the Thesis

Chapter 1 will provide a general introduction and state of the art followed by the research motivation, objectives, and a literature review. It will conclude with a technical discussion on aspects of machining critical to the comprehension of this study. Chapter 2 will discuss sample preparation, equipment, experimental procedures, and design of the experiment. Experimental results and observations are shown and discussed in Chapter 3. A summary of the study, as well as future work recommendations and conclusions are given in Chapter 4.

1.5 Review of Relevant Literature

Ductile iron was first discovered in 1948, around the same time that research was being conducted on the austempering of other ferrous alloys. Shortly after ductile iron was created it was austempered and studied. ADI was not used commercially until 1978

when Tecumseh used an ADI crankshaft in a hermetically sealed compressor. Following Tecumseh's lead, there was a flurry of attempts to use the material by automotive manufacturers. ADI saw use in differential ring and pinion gears, timing gears, camshafts, crankshafts, and other high wear applications. Following the initial rush of development, the interest and expansion of ADI died down due to machinability limitations [11].

Keough and Hayrynen [1] compared the raw mechanical properties of several alloys to ADI and noted that "fatigue strength of ADI is equal to or greater than that of forged steel" when compared to aluminum, steel, and ductile iron based on cost "ADI is the best buy per unit of yield strength". They explain the typical process of producing a component from ADI as "[ADI components] are cast in ferritic ductile iron at a nominal 150 BHN hardness, machined complete, austempered to about 450 BHN, cleaned and, (in some cases), seal ground" [1]. This article highlights the many applications of ADI in the automotive and heavy machinery industries, as well as the fundamental advantages ADI has over other alloys in its class. Their description of parts being cast, machined, austempered, and then ground to final geometry highlights the need to develop reliable methods of machining the iron after it has been austempered to reduce the number of steps and machine heat treated iron to its final net shape.

Handayani [12] noted an example of ADI replacing a steel assembly consisting of 84 individual pieces with a single casting. This is an excellent example of the potential ADI has to lower part complexity and cost while simultaneously improving durability. Examples like this were cited as motivation for the author to develop recommendations for cutting parameters in ADI using tooling that is readily available from manufacturers.

Handayani also discussed the need for future research to be conducted for the evaluation of threading operations in ADI.

Larumbe, Delgado, Alvarez-Vera, and Villanueva [13] analyzed the production of an ADI automotive component by forming, as opposed to casting. This method of production via plastic deformation of the material takes advantage of ADI's high ductility when compared to some other ferrous alloys with comparable toughness and wear resistance. The researchers utilized practical experiments as well as finite element modeling to determine that forming operations are a viable method of production in appropriate grades of ADI. While no examples of form tapping ADI could be found, the results of their research did demonstrate a practical example of adding value to an ADI component via plastic deformation.

Thread forming is called many different names such as form tapping, cold form tapping, cold roll forming, roll forming, thread rolling, roll tapping or cold roll tapping [9]. They all refer to the process of deforming the material into the shape of the threads rather than cutting it away. The mechanics of this process will be discussed more in depth in the next section.

Other types of cast iron are too brittle to form threads as they will crack during the operation. By leveraging ADI's ductility, form tapping would be an effective way to thread holes without wearing down a cutting edge on a tool. The plastic deformation of thread forming would also induce SIT of the material at the threads providing even more strength to the formed threads, which are stronger than cut threads due to grain deformation [9], [14]. Keough *et al.* [7] suggest that the transformative properties of ADI are precisely what would make thread forming the most difficult operation to complete.

Elosegui *et al.* [15] conducted a study examining the performance, lifespan, and power consumption of six different tap coatings for threading holes in grade 1 ADI with cut taps in a milling machine. The researchers noted that the ADI tends to adhere to cutting tools and primarily damages tools by a combination of adhesive and abrasive wear. Tools used on ADI exhibit significantly shorter service lives than when used on steels with comparable mechanical properties. The researchers also noted the lack of specific machining recommendations for ADI, specifically for tapping operations.

Many machining operations will pump an oil or water-based coolant onto the cutter/workpiece interface to reduce friction between the tool and the workpiece and to carry away chips and heat. This is done to minimize tool degradation and improve part surface finish [5], [16]. Minimum Quantity Lubrication (MQL) is an alternative cooling method that delivers a blast of compressed air with a small volume of atomized oil added to the stream. Sakharkar and Pawade [16] determined that MQL improved tool wear and surface finish in ADI machining as compared to both dry machining and flood coolant. It should be noted that these results were observed in turning operations which had direct access to the leading edge of the tool during the entire operation, this is not the case when drilling or tapping. Better results might be achieved in drilling operations by delivering coolant to the tip of the tool via through spindle coolant. Handayani [12] used this method for drilling ADI grades 1 and 3 with good results.

ADI is a relatively unknown material with an unparalleled combination of properties and cost. ADI's reputation as a material with poor machinability has reduced its utilization in many applications where its properties are superior to the alloy that was chosen due to the designer's preference for familiarity and ease of use. Modern advances

in tooling make machining ADI a possibility. The incomplete list of appropriate processes and parameters is an obstacle holding ADI back from replacing many existing steel and aluminum parts. Research conducted over the last decade has greatly improved our understanding of ADI machining, but a large portion of parameters remain unknown.

1.6 Discussion of Threading Methods

This section discusses the threading methods utilized in this study. The three methods that were utilized are the most common methods of producing threads. Two of the methods rely on synchronized tool rotation and axis motion. In situations where the machine accomplishes this by using closed-loop feedback to maintain this synchronization the tools can be held rigidly in a standard tool holder. This is referred to as rigid tapping. Specialized floating tap holders can be used to allow the tap to walk along the axis of the spindle in machines that do not have rigid tapping capabilities. The third method, thread milling, does not require tool rotation to correspond to axis motion and typically rotates at milling speeds uninterrupted for the entire operation. Selection of which method manufacturers choose to use in their process depends on several factors that are specific to the application.

1.6.1 Cut Tapping

Cut tapping is a threading method that utilizes a solid cutting tool with geometry designed to produce threads via shearing action. Cut taps are ground according to the thread form they are meant to produce and can only produce that thread form. Cut taps are the most common tool for producing threads from a drilled hole as they are the type of tap used in hand tapping with the user manually driving the tool with a tap wrench. A disadvantage of cut taps is that they produce chips during operation. The chips are

directed into the flutes of the tool but will quickly pack up if they are not evacuated from the hole [9], [14]. Chip packing will negatively influence tool life, but it can also result in catastrophic tool failure. There are three common tap flute geometries: straight flute, spiral flute, and spiral point. As the name suggests straight flute taps have flutes that run parallel to the tool axis, they do not direct the movement of chips and the taps are able to be ground with a larger core than the other two styles providing greater tool strength. Spiral flute taps have flutes that spiral upwards to direct chips out of the hole, similar to a twist drill bit. Spiral flute taps are preferred when tapping blind holes, especially when the material produces long continuous chips. Finally, spiral point taps are similar to straight flute taps but direct chips forward, deeper into the hole. They are excellent at threading through holes or holes where additional clearance can be drilled at the bottom of the threads [17].

This study utilized a straight flute tap because ADI tends to produce short, segmented chips. These chips break off into the flutes and are pulled down by gravity. The workpieces in this study were drilled through so chips were free to drop out the bottom of the test specimen. No special considerations were needed for chip management due to the machining setup for this experiment. The additional tool strength provided by the thicker core is a desirable benefit, particularly when tapping materials with high toughness [17]. Real world applications are likely to present a machinist with less-than-ideal threading conditions which could necessitate utilizing a different approach.

1.6.2 Form Tapping

Form tapping is another threading method that utilizes a solid tool ground to produce a single thread form. Form tapping differs from cut taps in that it does not shear

the material. No material is removed from the workpiece, it is plastically deformed into the shape of the threads. Because no material is removed, chip evacuation is not a concern which makes form taps excellent choices for deep (>3 x diameter) tapping applications. This also means form taps do not have flutes. Form taps are often ground with oil passages that look similar to straight flutes, but they only function to deliver lubrication to the tool and do not interact with the material [9], [14], [18].

Form taps have the added benefit of producing threads with greater strength than threads that are cut. This is due to the material flowing as it is deformed and aligning the grains of the matrix. This property is observed in threads formed in any material as it is a form of localized strain hardening [14]. A graphic illustrating the grain flow concept can be seen in Figure 1.1 at the end of this section. In addition to strain hardening the plastic deformation of the threads strains ADI past the point of martensitic transformation. This results in threads that have a greater concentration of martensite than the surrounding matrix, further improving thread strength [12], [19].

The primary concern regarding the viability of thread forming ADI was due to the ductility of the material. As a rule of thumb threads can only be formed in materials with a minimum of 9% elongation to fracture. Grade 1 ADI minimum specification for elongation meets this criterion. Grade 1 ADI, being the most ductile, was presumed to have the greatest chance of success. If grade 1 was found to be appropriate for thread forming, it would form the basis of future experiments investigating thread forming of the higher grades with poorer ductility [14].

1.6.3 Thread Milling

Thread milling differs from the other two threading methods by utilizing a rotating cutting tool instead of synchronized movement between the spindle and the feed axis. The tool rotates continuously at milling speeds and removes material in a series of small engagements. The profile of the cutting teeth matches the cross section of the thread (60º included angle for a standard thread form). This cutting profile is fed through the hole in a helical motion that matches the pitch and major diameter (compensating for the radius of the cutter) of the thread that is being cut [10].

Thread milling is more versatile than the tapping methods as a cutter with a single cutting point can produce any thread form provided the tool can fit into the minor diameter of the hole and the cutting teeth can reach the major diameter without rubbing the neck of the tool on the minor diameter. Helical profiles can even be programmed along a taper to accommodate tapered thread forms. Generally, thread milling requires multiple passes, and the helical motion of the tool is longer and slower than synchronized tapping. Thread milling cycle times can be improved by using cutters with multiple sets of cutting teeth. These cutters reduce the number of helical rotations the machine must complete to finish the length of the thread. The disadvantage being thread mills with more than a single cutting point are ground to a specific pitch and can only cut threads that match that pitch.

An example would be a thread mill with 10 sets of teeth along a 20 threads per inch (TPI) pitch could be used to cut both a 1/2-20 thread, and a 7/16-20 thread while only requiring 10% of the feed motion of a cutter with only one cutting point. They could not be used to produce threads with a different pitch, and they require a greater amount of

rigidity from the machining setup as the increased material engagement will result in more tool deflection and cutting forces along the plane normal to the spindle axis.

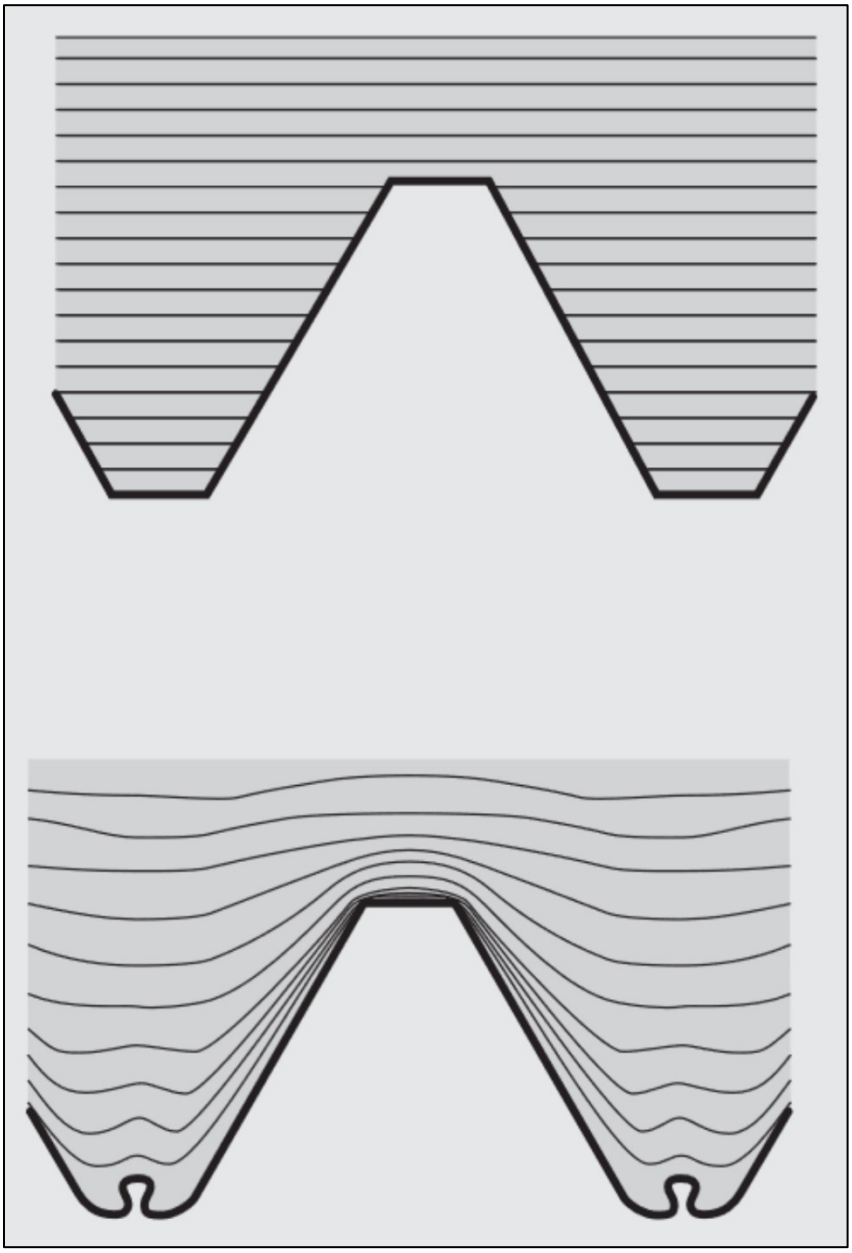

Figure 1.1: Grain structure of material matrixes after threading. The matrix of the cut thread (top) is disrupted by the material removed from the threading operation. The matrix of a formed thread (bottom) shows the material matrix flowing along the path of the thread. Note the channel formed by the small curls at the apex of the thread crest [18].

1.7 Discussion of Feeds and Speeds

This section will briefly discuss feeds and speeds as they pertain to recommended machining parameters.

1.7.1 Feed

Feed rate is a distance covered by the machine in a given amount of time. Machines are programmed in inches per minute or millimeters per minute for standard 3-axis motion. As feed relates to cutting parameters it becomes slightly more complex. Feed rate is the distance a tool advances with every passing of a cutting tooth, essentially how big of a bite of material a single tooth on the tool is supposed to take. Too large and you can overload the tool, too small and the tool will fail to dig in and produce a chip, it will deflect off the material and rub. Over or under engaging can both result in inaccurate dimensions, poor surface finish, chatter, accelerated tool wear, and tool breakage. When starting recommendations for cutting parameters are provided, they are given in feed per tooth (FPT); this is also known as the chip load. The value that is programmed into the machine is then calculated based on the rotational speed of the tool, and the number of flutes the tool has. If a family of tools is offered with a variety of number of flutes, a manufacturer may only need to provide a single chip load for a given cutter-workpiece combination [5].

1.7.2 Speed

Machines are programmed in spindle speed, measured in rotations per minute (RPM). Like with feed, the speed recommendation that is provided for a given tool is a blanket value that often applies to a range of tools within a family. Speed is provided in surface feet per minute (SFM) which is the speed the edge of a cutting tooth is traveling.

A larger diameter tool will have a higher SFM than a smaller diameter tool if they are turning at the same RPM. Therefor if tools within the same family are prescribed the same SFM moving to a smaller diameter requires running a faster spindle speed to maintain the same speed that the cutter is pushed through the material. As discussed in the previous section feed rate is influenced by spindle speed, and spindle speed is influenced by cutter diameter. The values are intertwined and modifying speed directly impacts the programmed feed rate of the machine [5].

All of this is to say that tooling manufacturers and feeds and speeds databases provide information that describes how the cutting edge of the tool should interact with the workpiece and calculations that account for tool geometry are required to program a CNC machine. The topic of feeds and speeds is more complex than what was discussed here, this section is only meant to be a brief summary of the values provided by tooling references.

2. MATERIALS AND METHODS

Test specimens were cut from a single bar of continuously cast ductile iron. They were then austempered to a grade 1 ADI, and a combination of various manufacturing methods were used to thread holes into the blocks. Data collected during and after the process includes cutting force measurements, surface profilometry, and micrographs of the specimens. Details are presented in the sections below.

2.1 Ductile Iron

2.1.1 Material Acquisition

The material utilized in this study was Dura-Bar 65-45-12 ductile cast iron. The bar was shipped from Dura-Bar in Woodstock, IL. All test pieces in this study were cut from the same cast bar on a horizontal band saw. This was done to ensure uniformity of chemical composition and casting conditions for the specimens. The as-received iron was cast as a 3.25 in x 6.25 in x 72 in bar and the sides were milled down to 3.030 in x 6.030 in ± 0.010 in by Dura-Bar to improve overall grain size and matrix uniformity. As the edges of the casting cool quickly they form a different grain structure and matrix than the rest of the bar. This effect can be seen by the material certification data provided by Dura-Bar. Table 2.4 shows a variation of hardness, and Table 2.1 shows a difference in pearlite formation from the center to the edges of the casting. Hardness values of the as-cast iron were confirmed upon delivery of the bar; observed measurements can be found in Table 2.5. Given the nature of casting production, the effect of matrix non-uniformity due to differential cooling rates cannot be eliminated entirely, but by removing the outer casting surface of the bar the impact of this phenomena on the test sample was

minimized. Grain size uniformity is a characteristic that also lends itself to austemperability [3].

Table 2.1: 65-45-12 Iron Matrix Composition and Nodule Count

Microstructure	Pearlite %	Ferrite %	Carbide%	Nodule Count (per mm^2)	Nodule %
Edge	0	100	0	100	97
Center	30	70	0		

2.1.2 Properties

All specimens observed in this study were produced from a single cast bar possessing the chemical composition shown in Table 2.2. The sample conforms to ASTM A536 grade 65-45-12 standards. Tensile properties and hardness values from the material certification provided by Dura-Bar can be found in Table 2.3. and Table 2.4.

Table 2.2: Chemical Composition of Iron Bar

Chemical	Wt. Percent
Carbon (C)	3.66
Phosphorus (P)	0.018
Sulfur (S)	0.014
Manganese (Mn)	0.25
Silicon (Si)	2.678

Table 2.3: Tensile Properties of 65-45-12 Iron Sample

Material Property	Observed Value
Tensile Strength	69 300 psi
Yield Strength	50 000 psi
Elongation	19%

Table 2.4: As-Cast Iron Bar Hardness Certification

Location	Min Hardness (BHN)	Max Hardness (BHN)
Edge	179	191
Center	182	203
Mid-Radius	177	189

2.1.3 Sample Preparation

The milled bar was received and fed lengthwise into a horizontal bandsaw where the final 3 inches of the bar were removed and discarded, and then nine samples, each approximately 0.82 in. thick, were sectioned off. The saw-cut faces of the specimens were then milled on a Bridgeport style manual milling machine. A 3.5 in. diameter shell mill was used to cut the faces in a single pass. Once the saw cut faces were machined parallel to one another, each specimen was reduced to a thickness of 0.75 in. ± 0.002 in. The blocks were stamped 1A through 8A for identification purposes, one specimen was marked 4B to be used as a spare in the event of one of the primary eight specimens being invalidated throughout the study. Next, the specimens were cleaned, weighed, and measured at five points across the thickness; two points along the length, and one point along the width. Thickness measurements were taken with a 0-1 in. digital micrometer

with a minimum resolution of 0.00005 in. Length and width measurements were recorded with a pair of 6 in. digital calipers with a minimum resolution of 0.0005 in. A diagram depicting the sample and measurement points can be seen in Figure 2.1.

Specimens 1A through 4A were loaded into the CNC milling machine and drilled with the corresponding tap drill in the as-cast state, and the four samples were once again cleaned and weighed. Sample dimensions and hole pattern can be seen in Figure 2.2. The nine prepared samples were sent to Applied Process where they were austempered to a grade 1 ADI. Once the samples returned, they were remeasured and compared to the original values to determine how much dimensional change the heat treatment imparted on the specimens.

The austempered specimens were then tested for hardness at five points for average comparison to the as-cast state. Austempered sample hardness measurements can be found in Table 2.5. The hardness of the specimens aligns with the expected hardness range of a grade 1 ADI as defined by ASTM. Figure 2.3 is an image of the microstructure of the austempered iron after heat tinting. Details of the metallographic and heat tinting process are presented in Section 2.7

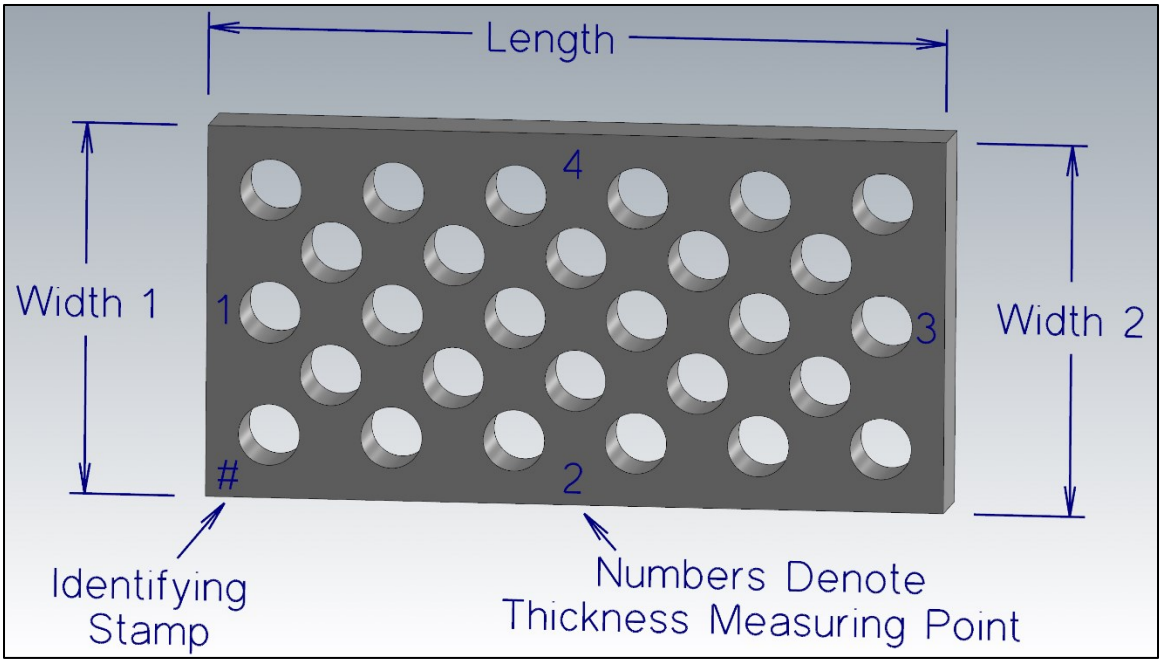

Figure 2.1: Points of measurement on test specimens. Points were used for quantifying sample growth from the austempering process.

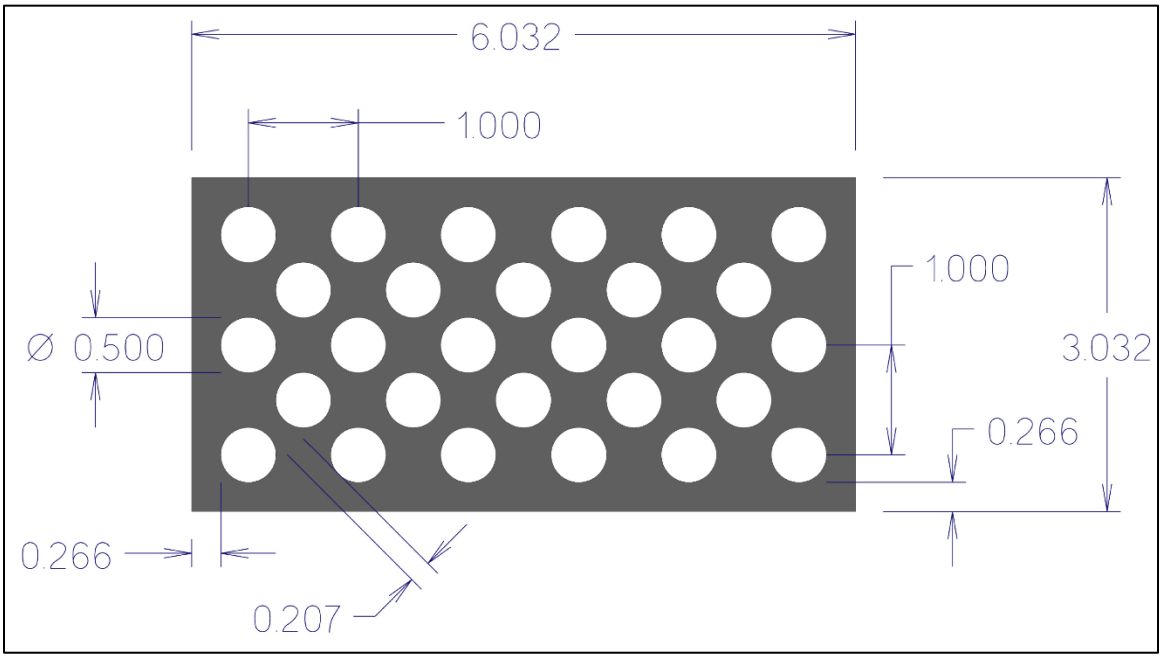

Figure 2.2: Specimen block dimensions and threaded hole pattern.

Table 2.5: Average Hardness of Iron Samples

Sample	Average Hardness (BHN)	Standard Deviation
As Cast	174	11.13
1A	321	7.07
2A	323	4.47
3A	315	5.48
4A	311	0.00
5A	300	4.02
6A	302	6.36
7A	300	4.02
8A	300	4.02
4B (Extra)	298	4.93

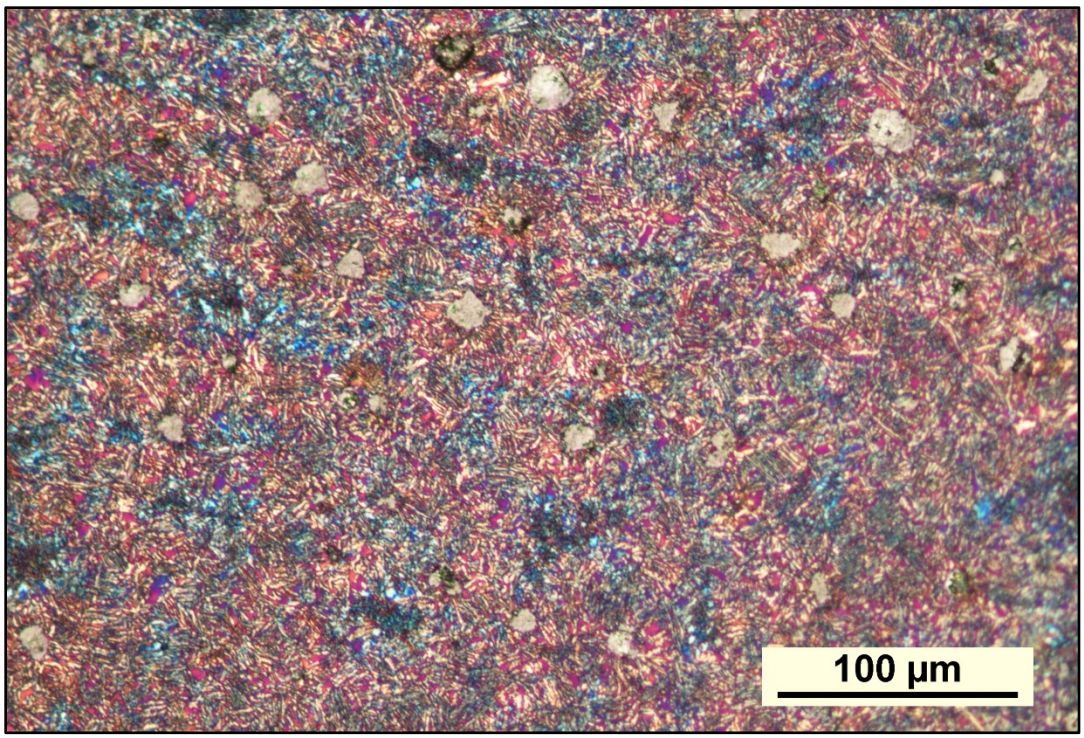

Figure 2.3: Heat tinted microstructure of sample 4B. Colors imparted by the heat tinting process can be used to identify the constituents of the ADI matrix.

The image above shows the typical matrix of the ADI after polishing and heat tinting. The beige circular structures are graphite nodules suspended in the acicular matrix of ferrite, which is straw colored, and austenite. The retained austenite is present as both violet and light blue color. The violet is stabilized austenite, and the light blue is high-carbon metastable austenite. When the material undergoes sufficient deformation SIT will occur and the metastable retained austenite will transform into martensite which would appear in heat tinted samples as a dark blue color.

2.2 Cutting Tools

The tools utilized in this study were commercially available options from established tooling manufacturers. Carbide-tipped indexable tooling was selected where

available for improved abrasion resistance. Coated tools were selected when available for improved wear resistance. A list of the tools used in this study can be found in Table 2.6.

The tools in this study were run at the feeds and speeds recommended by the tooling manufacturer. Kennametal was the only manufacturer to provide a recommendation for feeds and speeds in the catalog for K3 materials, the subclass of irons that contains ADI. All other manufacturers had to be contacted for technical support and recommendations. The feeds and speeds used for each tool is listed below in Table 2.7.

The thread mill was run at 200 SFM with a chip load of 0.00106 IPT. A series of calculations were performed to convert the feeds and speeds provided by the manufacturer into values that would be programmed into the machine. To do this, Equation (2.1) was utilized to determine the spindle rpm to be programmed.

$$RPM = \frac{SFM \times 3.82}{\theta} \tag{2.1}$$

Where Θ is the diameter of the cutter in inches. Once spindle RPM is known, feed rate is determined using Equation (2.2)

$$F = RPM \times IPT \times N \tag{2.2}$$

Where F is the programmed feed rate in inches per minute, and N is the number of teeth on the cutter. Finally, the calculated linear feed rate was adjusted to compensate

for the cutting diameter of the tool being close to the diameter of the hole being milled with Equation (2.3).

$$F_{adj} = \frac{\theta_{major} - \theta_{cutter}}{\theta_{major}} \times F \tag{2.3}$$

Where F_{adj} is the compensated feed rate that is to be used on the program, Θ_{major} is the major diameter of the thread being cut, Θ_{cutter} is the diameter of the cutting tool, and F is the linear feed rate found in Equation (2.2).

Table 2.6: Tools Utilized in the Study

Item	Description	Manufacturer	Item Number
KenTIP FS Modular Drill Body	31/64in 5xD Indexable Drill Body	Kennametal	6372027
KenTIP FS Modular Drill Body	15/32in 5xD Indexable Drill Body	Kennametal	6372026
KenTIP FS HPG Carbide Drill Insert	31/64in Modular Drill Insert	Kennametal	6388734
KenTIP FS HPG Carbide Drill Insert	15/32in Modular Drill Insert	Kennametal	6388726
LMT-Fette Indexable Tap Body	Indexable Tap Body	LMT-Fette	9115328
LMT-Fette Forming Tap Inserts	Carbide Thread Forming Inserts	LMT-Fette	7248876
OSG Cut Tap	Powdered Metal Straight Flute Cut Tap	OSG Tools	1005201608
Harvey Tool Thread Mill	Single profile 4 flute solid carbide thread mill	Harvey Tool	54270-C3

Table 2.7: Feeds and Speeds of Tools on ADI

Tool	Feed (IPT)	Speed (SFM)
Kennametal 31/64 in. drill	0.00350	260
Kennametal 15/32 in. drill	0.00350	260
OSG Cut Tap	0.01250	25
LMT Forming Tap	0.01250	29
Harvey Tool Thread Mill	0.00106	200

2.3 CNC Mill

The milling machine used in this study was a Haas VF-2YT vertical machining center. The machine is configured with a 30 HP spindle capable of 8 100 RPM, a wireless probing system, and MQL system. Wireless probing provided a fast, accurate, and repeatable solution for setting work offsets. MQL was selected for tool lubrication and chip evacuation as a through-tool coolant delivery method was not within the capabilities of the equipment. MQL showed good performance in some of the research literature, and cutting oil was the lubrication recommended by the tap manufacturers. The MQL system delivered 0.82g of cutting oil per minute at 73 psi.

2.4 Dynamometer

Cutting forces for drilling and threading operations performed in the CNC mill (details provided in Section 2.4) were captured on a Kistler type 9170A rotating 4-component dynamometer tool holder shown in Figure 2.4. This device sampled force along the tool's X,Y, and Z axis as well as torque about the rotational axes. In addition to capturing cutting forces at the tool-workpiece interface, the dynamometer, being the rotating type, doubled as the tool holder. The 9170A is a modular design which can

accept a variety of tapers and ER collet systems to be fitted to the most common machines and tools found in the metalworking industry. To interface with the mill, the dynamometer was fitted with an ANSI / ASME B5.50-40 (CAT 40) single contact taper and an ER-40 collet system capable of accepting tooling with a maximum shank diameter of 1.024 in. Straight shanked tools such as the drills and the thread mill were held with a ½ in collet while the rigid tapping tools with square drives at the end of the shank were held with tap collets to provide maximum clamping force on the tool to prevent slipping and pull out, which would result in desynchronization between the rotation of the tool and the Z axis.

Sampling frequency was determined using Equation (2.4)

$$f_{toothpassing} = \frac{n}{60} * N \tag{2.4}$$

where $f_{toothpassing}$ is the frequency at which a cutting edge engages the material (the frequency of interest), n is the programmed spindle speed in rotations per minute (RPM), and N is the number of cutting teeth on the tool.

The frequency of interest was then multiplied by a factor ranging between 5 and 10 to determine the sampling frequency for the data run that would not overlap with the system's natural frequency, as recommended by Kistler. Table 2.8 contains information detailing the tool, process, parameters, and sampling rate frequency for the operations captured in the study.

Figure 2.4: Kistler Type 9170-A rotating dynamometer with carbide insert drill.

Table 2.8: Operation Feeds, Speeds, and Frequencies

Operation	Number of Teeth	Spindle Speed (RPM)	Feed Rate (IPM)	Frequency of Interest (Hz)	Sampling Factor	Sampling Frequency (Hz)
As-Cast 31/64ths Drill	2	2 839	19.87	94.63	7.5	710
Austempered 31/64ths Drill	2	2 050	14.35	68.33	10	684
As-Cast 15/32nds Drill	2	2 933	20.53	97.77	7.5	734
Austempered 15/32nds Drill	2	2 118	14.8	70.60	10	706
Thread Cut Tapping	4	191	9.55	12.73	10	128
Formed Thread Tapping	5	229	11.45	19.08	10	191
Thread Milling	4	1 969	1.85	131.27	10	1313

2.5 Experimental Procedures

Samples were loaded into the mill and held with a Kurt AngLock 8-in 3-axis vise which was bolted to the table lengthwise. The stationary jaw was trammed to the machine's Y-axis. The lower corner where the sample is stamped for identification was placed face-up against the stationary jaw of the vise closest to the operator and was used as the reference point for all operations. Once the sample was held in the mill the reference corner was probed to set the work coordinate system (WCS) for the program as

seen in Figure 2.5. Programming for the operations was done using Mastercam. Images of the programming environment can be seen in Figure 2.6 and Figure 2.7 below.

Forces during all machining operations performed on the samples were captured using the dynamometer. Samples that were not drilled prior to heat treatment were first drilled with the corresponding tap drill. Austempered samples were drilled with new inserts for wear and force comparisons to samples drilled in the as cast state. Figure 2.8 shows the experimental setup prior to a drilling operation. Once drilling was complete, the rotating dynamometer was removed from the spindle and fitted with the threading tool that was prescribed for the sample loaded in the mill. The threading tool was touched off on a tool setting probe to set the tool offset in the machine while the X- and Y- work offsets remained unchanged.

Removing the predrilled samples from the machine between the threading and drilling operations introduces the possibility of slight misalignments between the two operations. This could potentially accelerate wear on the threading tool, produce threads that are out of tolerance, or cause catastrophic failure of the tool. It is preferable to drill and tap in a single setup to eliminate this potential for error and to reduce spindle down time dedicated to setting up a part multiple times. These disadvantages are innate to the drilling-before-heat-treatment approach and should be considered by the manufacturer.

Specimens were threaded with their prescribed threading method and then were removed from the mill and cleaned. Threads were checked for damage and function, and finally the blocks were sectioned for evaluation.

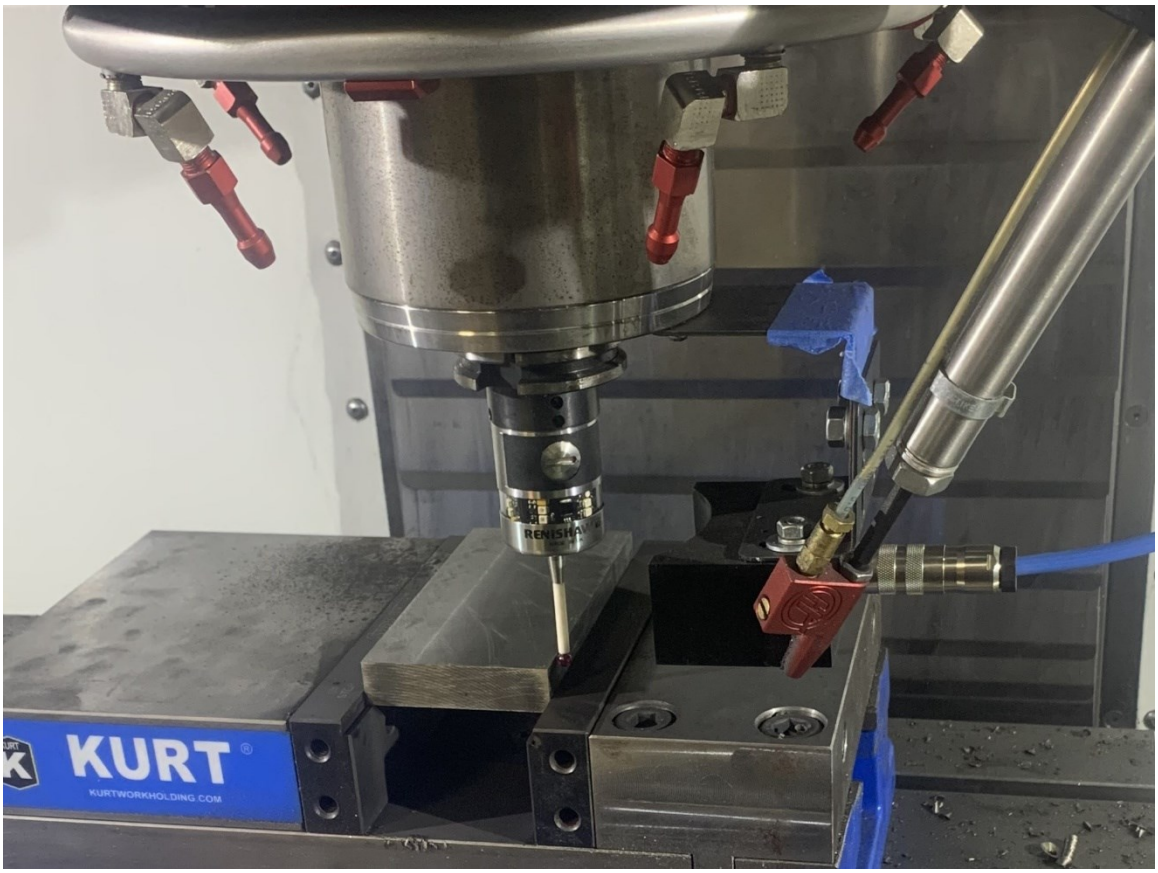

Figure 2.5: Probing a specimen to establish the WCS for the CNC operation.

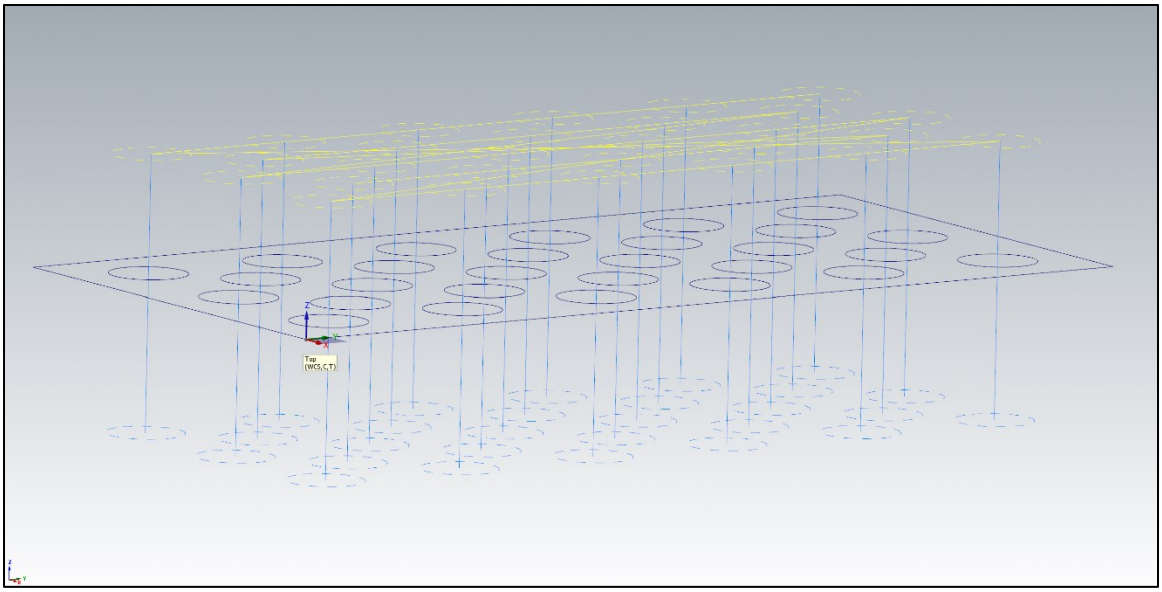

Figure 2.6: Mastercam programming environment with drilling/tapping operation movements displayed.

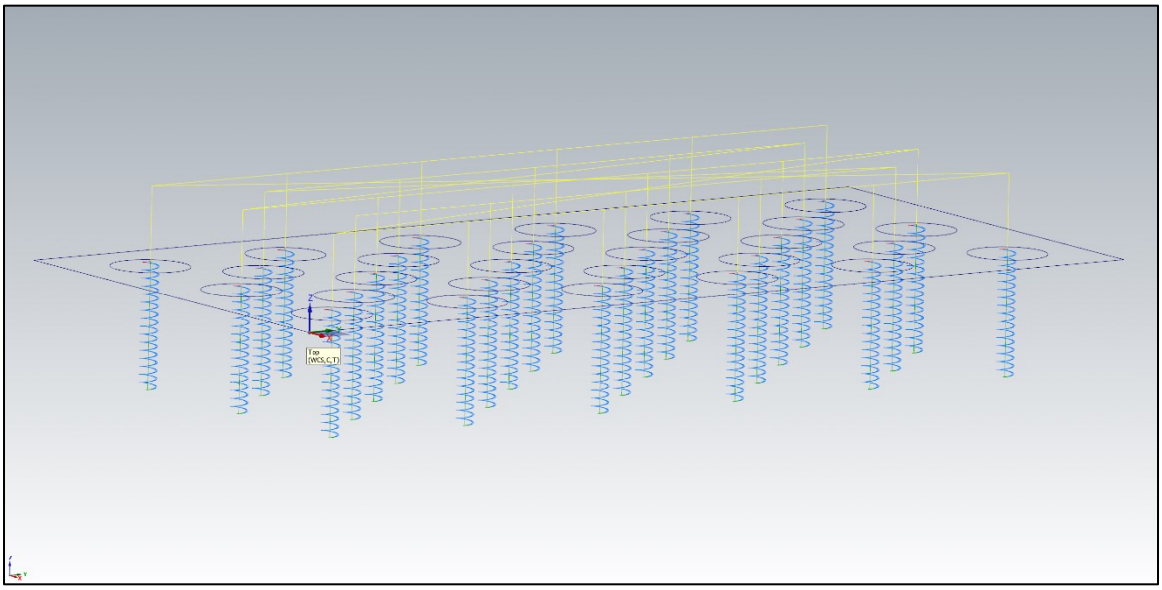

Figure 2.7: Mastercam programming environment with thread milling operation movements displayed.

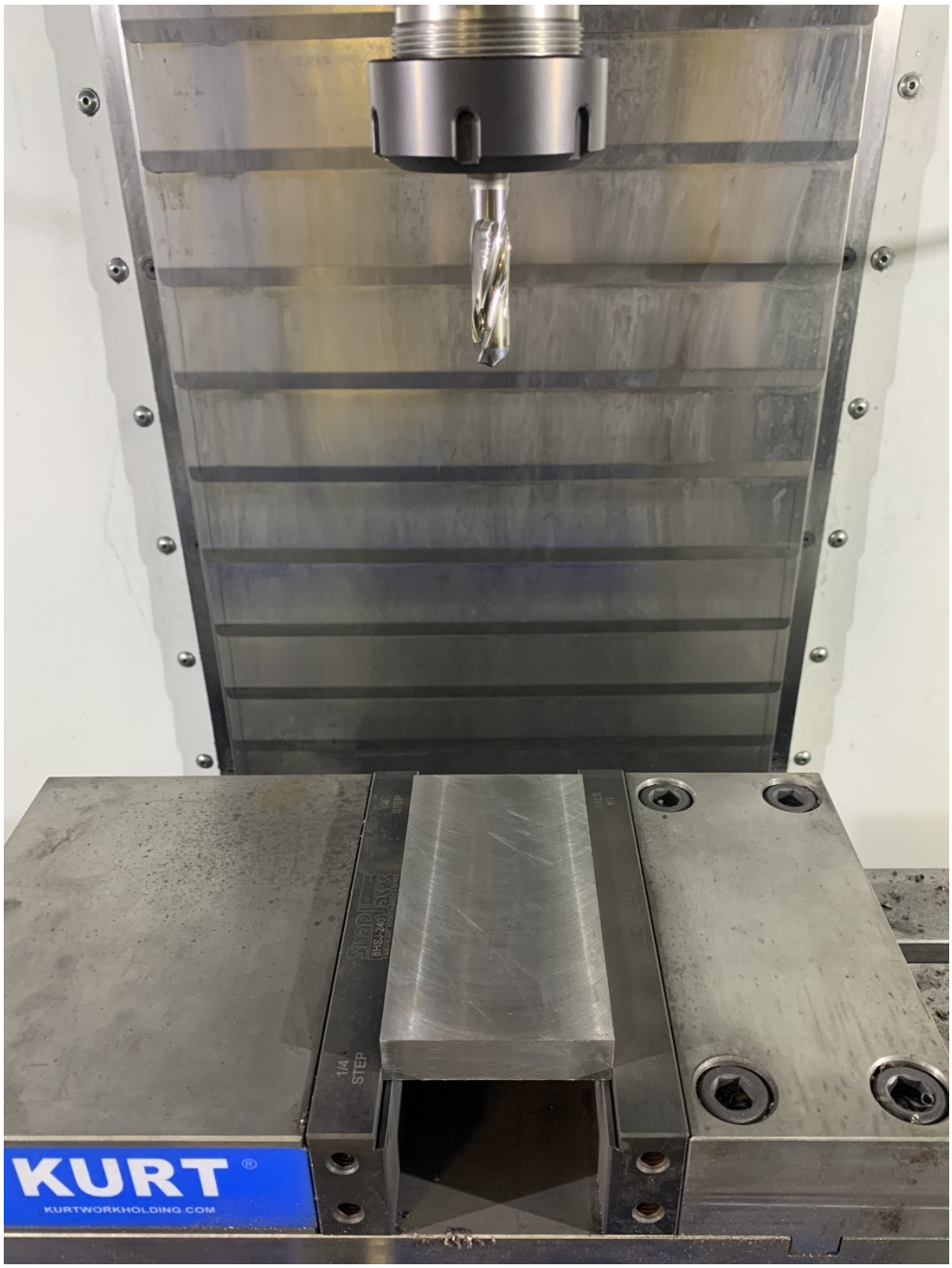

Figure 2.8: Experimental setup for drilling operations.

2.6 Design of Experiment

The design of the experiment regarding sample heat treat condition when drilled, tap drill size, and method of threading can be found in Table 2.9. Sample 4B was

intended to be a backup sample produced from the same bar and heat treated under the same conditions as the primary eight samples. All eight samples were successfully machined without incident. Therefore sample 4B was used to test the viability of thread forming at a greater percentage of thread formation.

Table 2.9: Design of Experiment

Sample Number	Heat Treat Condition when Drilled	Tap Drill Diameter	Threading Method
1A	As Cast	31/64 in.	Formed
2A	As Cast	15/32 in.	Cut Tap
3A	As Cast	15/32 in.	Thread Mill
4A	As Cast	31/64 in.	Formed
5A	Austempered	31/64 in.	Formed
6A	Austempered	15/32 in.	Cut Tap
7A	Austempered	15/32 in.	Thread Mill
8A	Austempered	31/64 in.	Formed
4B (Spare)	As Cast	31/64 in.	Formed (75% thread formation)

2.7 Characterization

Cross-sectioned holes that were drilled and threaded in the order of 1-13-7 for each block were scanned in a Keyence wide-area 3D measurement system optical profilometer for a comparison of thread surface finishes across the various threading operations. Optical images of the scans can be found in Figure A.1 through Figure A.8 in the appendix. Hole number 1 was sectioned off and mounted for metallographic

characterization. Specimens were ground and polished using standard metallographic techniques. They were then etched with a 2% nital solution for approximately 8 seconds before being rinsed and dried. After etching, the specimens were broken out of their mounts and placed in a heat proof container with the polished surface facing up. This container was placed in a furnace at 500°F with an air atmosphere for 5 hours and then removed and left to cool in still air. After heat tinting the samples were viewed under magnification and the primary constituents of the ADI matrix were differentiated by the color imparted by the heat tinting process.

3. RESULTS AND DISCUSSION

3.1 Observations

3.1.1 Dimensional Changes in Samples

Dimensional changes in the iron specimens due to the phase changes associated with austempering the iron were expected and observed. Dimensional growth is affected by the ratio of ferrite to pearlite in the as-cast iron [12]. Tight process control begins with the chemistry of the iron and the way it is initially cast. Quality iron from the very beginning can enable a manufacturer to develop a process that designs around a parts growth and still maintains tight tolerances [3], [12].

The samples in the study grew at an average rate of 0.00086in/in. Table 3.1 shows average dimensional change between the as-cast and austempered state for each sample. Raw data for sample growth can be found in Table A.1, a diagram depicting the points of measurement on the test specimens can be found in Figure 2.1.

Table 3.1: Observed Iron Growth after Austempering

Measurements	All Specimens	Predrilled Specimens	Solid Specimens
Overall Average Gowth (in/in)	0.0009	0.0009	0.0009
Growth Measurements Perpendicular to Hole Axis (in/in)	0.0007	0.0009	0.0006

3.1.2 Tool Wear

Comparable tool wear was noted among all the tools used in this study. Mild crater wear was present on the rake of the thread cutting tools after 28 holes, and on the apex of the lobes of the forming tool and the rake face of the drills after 56 holes. Images of the tools can be seen in Figure 3.1 through Figure 3.9 below.

A relationship between class of thread fit and tool degradation was beyond the scope of this study; all tooling was rated to produce a class 2B threaded hole by their respective manufacturer. It should be noted that a standard grade 5 zinc plated fastener with a class 2A fit was successfully threaded into all holes produced across the study.

Comparative tool life for the different threading tools and methods was not evaluated as the number of holes produced was insufficient to be statistically representative of a tool type. Under the threading conditions established for the study none of the tools were used to the point of developing significant wear or undergoing catastrophic failure, and all holes produced accepted a class 2A bolt.

3.1.3 Catastrophic Tool Failure

At the conclusion of the study the unused spare test specimen (4B) was used to test the viability of forming threads to greater thread formation percentages. The 28 holes were first drilled with the 15/32nds drill bit which would have resulted in 92% thread formation. Next, the first 26 holes were milled using an endmill to interpolate a hole diameter of 0.475 in which would produce threads with 75% formation. The final two holes were interpolated to 0.471 for 85% thread formation. Holes at 75% formation were successful, however the tool was subject to forces significantly greater than those

observed at 50% formation in the rest of the study. Forces are discussed and in the next section, data can be found in Table 3.2.

The tool failed catastrophically when attempting to form threads at 85%. This result was anticipated as thread formation beyond 75% in any application is generally not advised due to the dramatic increase in cutting forces, and a corresponding marginal improvement in thread strength [5].

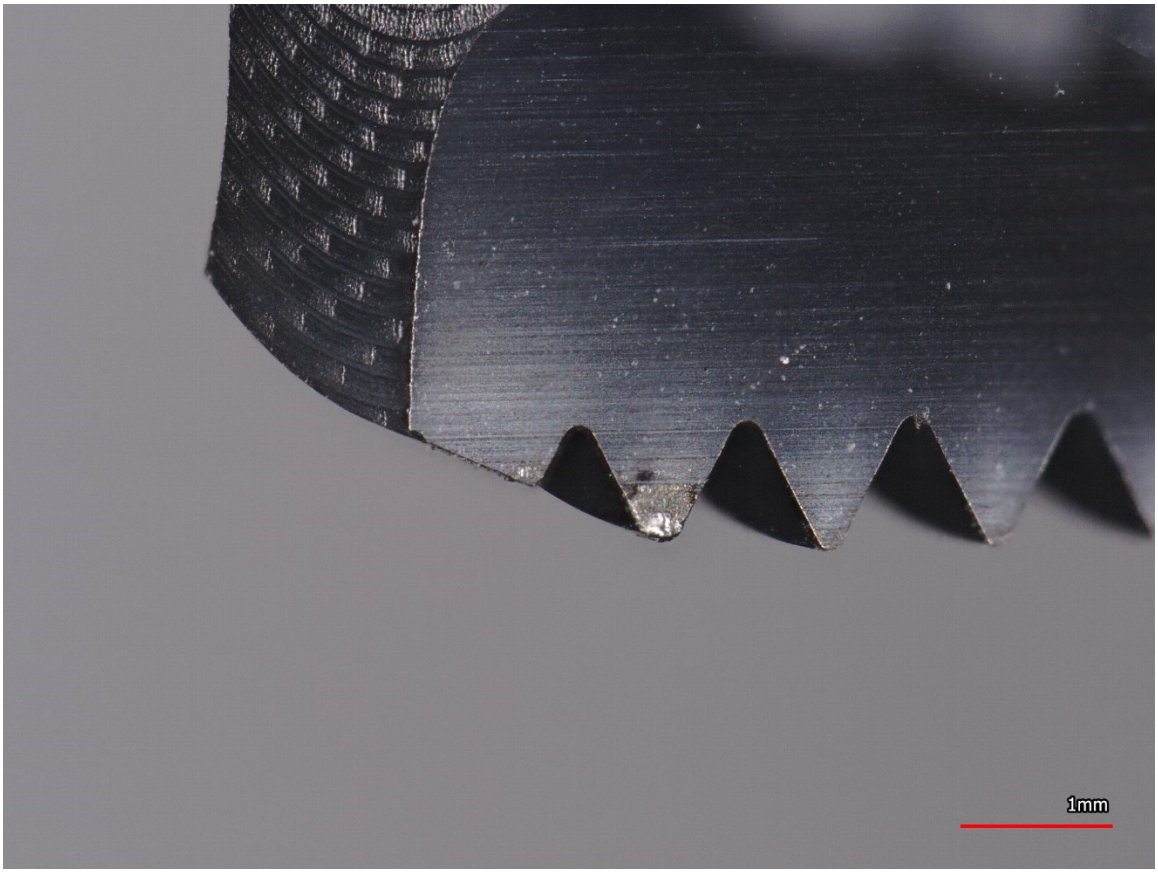

Figure 3.1: Light microscopy image of cut tap flute number 4 wear after 28 holes.

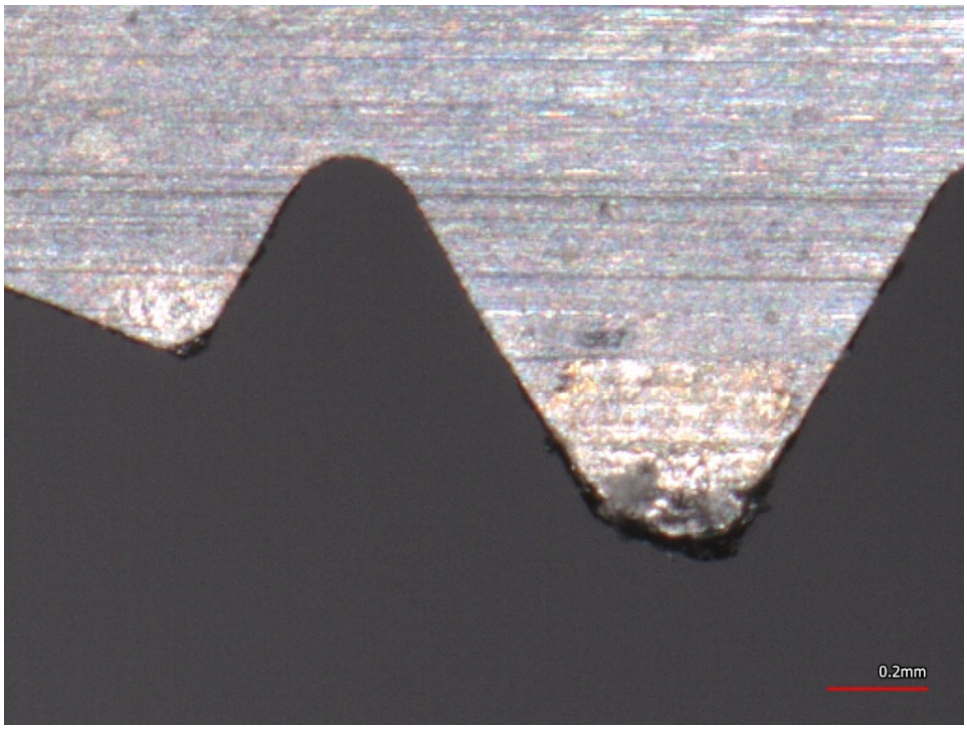

Figure 3.2: Cut tap flute wear after 28 holes. Crater wear is visible on the tool rake face.

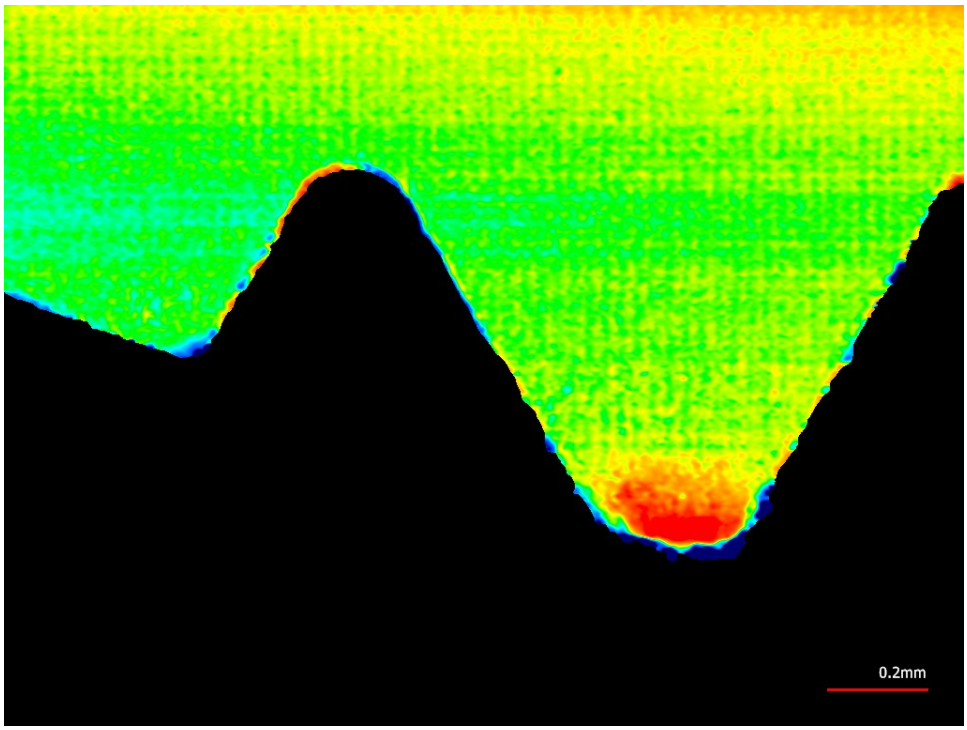

Figure 3.3: Topographical image of cut tap flute 4 after 28 holes. Wear is evident in the red region.

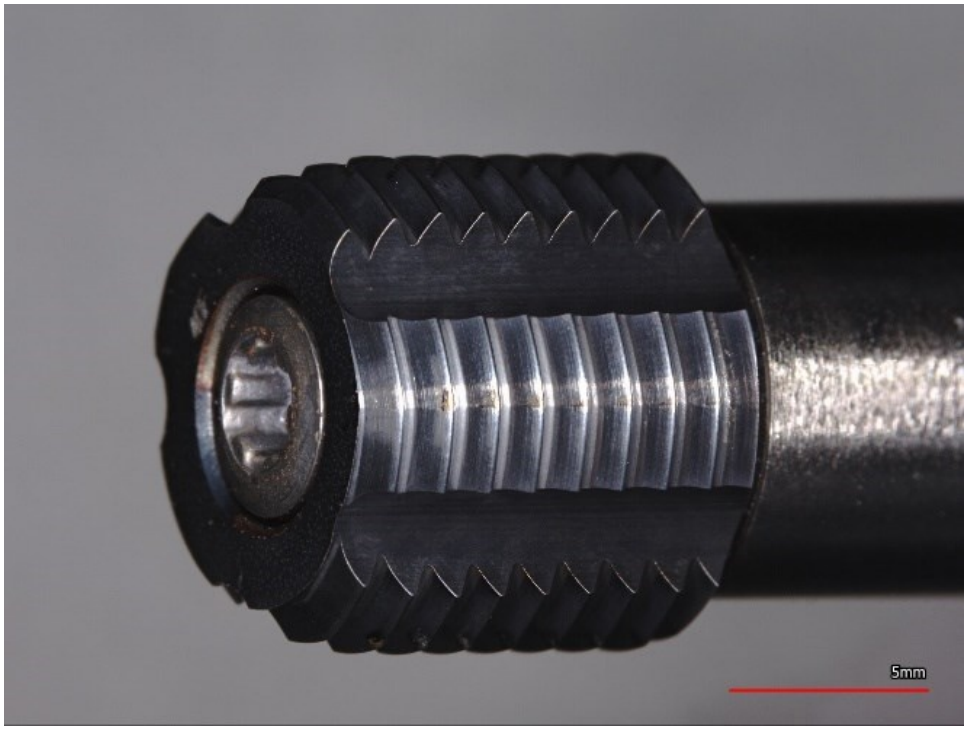

Figure 3.4: Lobe wear on the form tap insert after 28 holes.

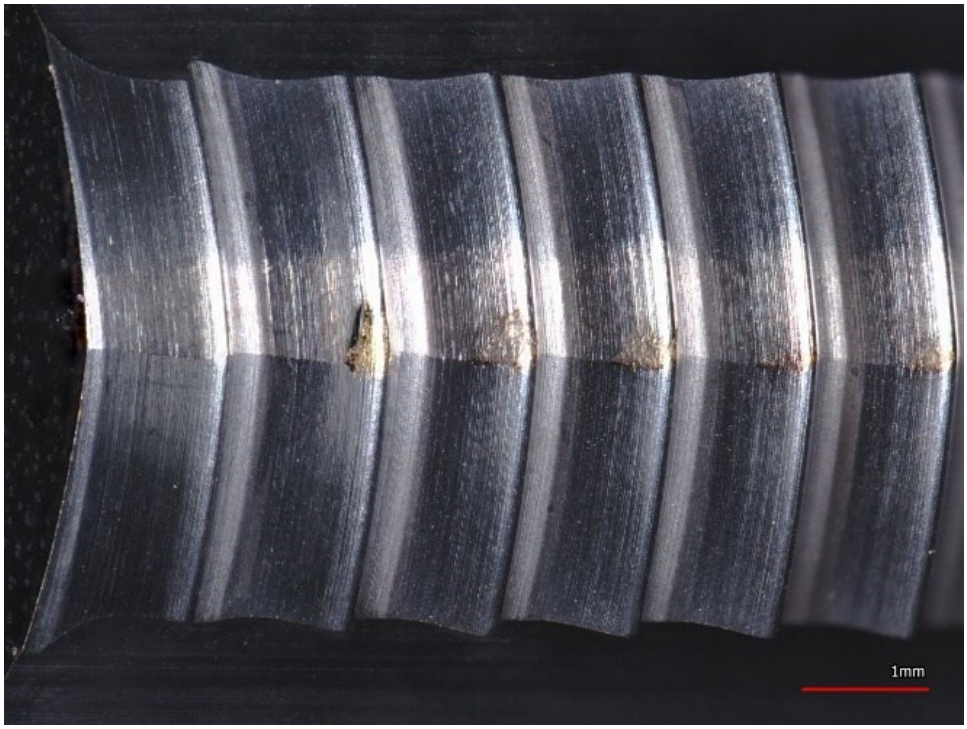

Figure 3.5: Form tap lobe wear after 28 holes.

Figure 3.6: Form tap lobe wear after 28 holes. Appears to show less wear than the flutes of the cut tap.

Figure 3.7: An unused carbide drill insert. Cutting rake face on the left side.

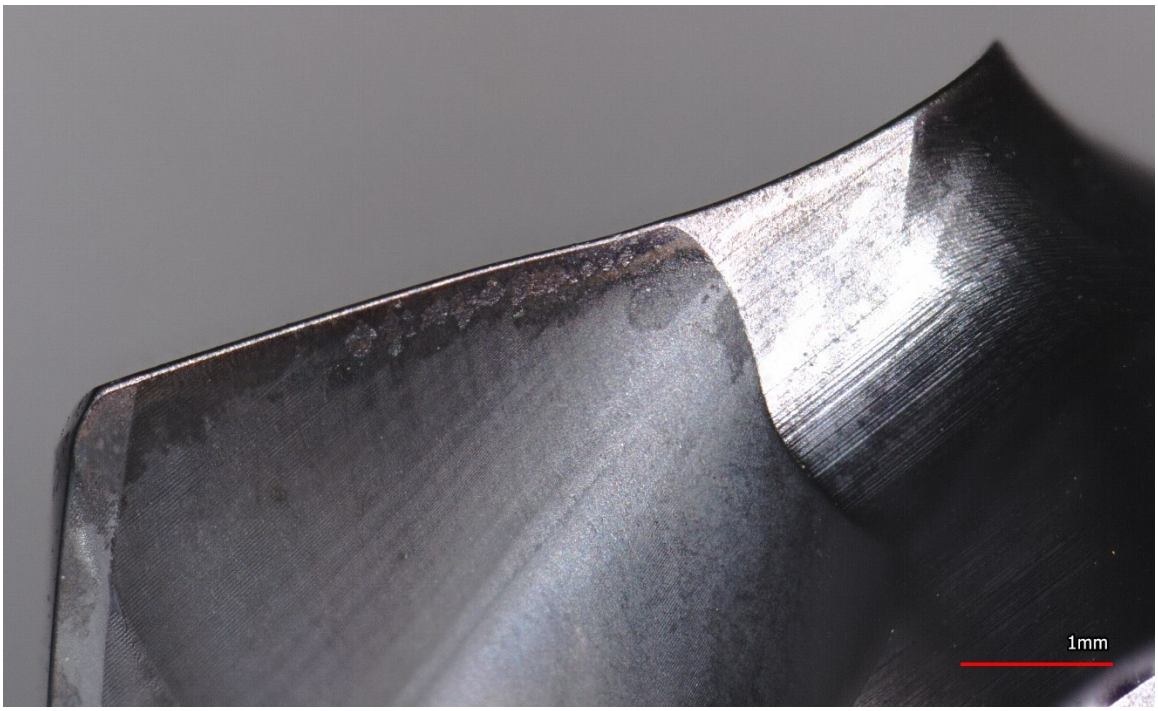

Figure 3.8: Drill insert rake face after 56 holes in ADI. Minor pitting beginning to appear.

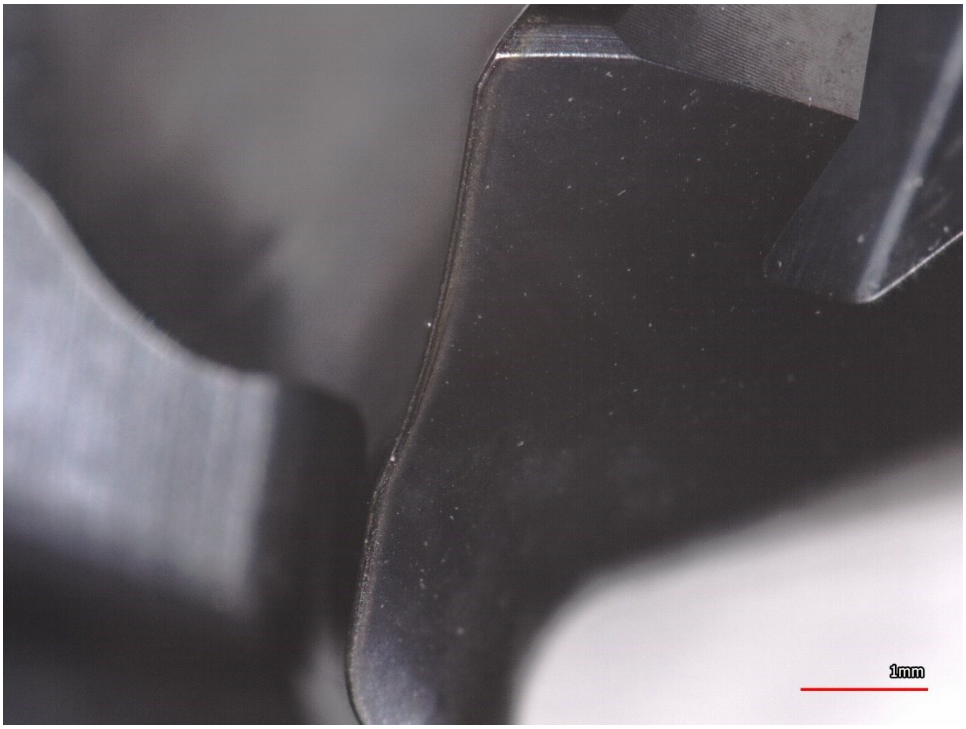

Figure 3.9: Drill insert flank after 56 holes in ADI. Less wear is present on the flank than on the rake face.

3.1.4 Dynamometer Data

Cutting forces, primarily force along Z and torque, observed in thread forming were higher than those in cut tapping. This result was expected due to the work required to plastically deform and displace the entire threaded region of the ADI matrix being greater than the amount of work required to shear the material in a cutting operation. The forces generated in the thread milling operations were extremely low and were confounded by noise produced by the data acquisition system while rotating at the cutting speed. Thread milling force data was not considered during later data analysis. Table 3.2 contains average and standard deviation values for maximum torque and standard deviation of the integrated torque curve per hole. Average work per hole was calculated using integrated torque and rpm in Eq (3.1).

$$J = \frac{I \times RPM \times \pi}{60} \tag{3.1}$$

Where J is the work done in joules, I is the integrated torque curve of the operation, and RPM is the spindle rotational speed in rotations per minute.

Table 3.2: Torque Values Observed in Rigid Tapping Operations

Specimen	Conditions	Average Max Torque (Nm)	Max Force Std. Dev.	Average Work (J)	Integral Std. Dev.
1A	Predrill/Formed	7.584	0.730	297.136	2.256
2A	Predrill/Cut	4.613	0.448	192.959	1.775
4A	Predrill Formed	7.024	0.934	289.875	2.283
4B	Predrill/Formed 75%	39.066	2.147	1507.594	11.631
5A	Postdrill/Formed	12.759	3.403	410.232	5.193
6A	Postdrill/Cut	4.506	0.216	193.892	0.717
8A	Postdrill/Formed	11.919	2.343	427.165	5.297

3.1.5 Chip Morphology

Both the as-cast ductile iron and the ADI tended to produce short, segmented chips. During drilling longer continuous chips in a continuously tightening curl were occasionally observed. Serrations could be seen at the inner edges of these chips. ADI specimens were drilled at 260 SFM and 0.0035 IPT which is in the middle of the range of the manufacturer recommendations of 160 to 330 SFM. Images of the chips formed while drilling can be seen below in Figure 3.10 through Figure 3.15.

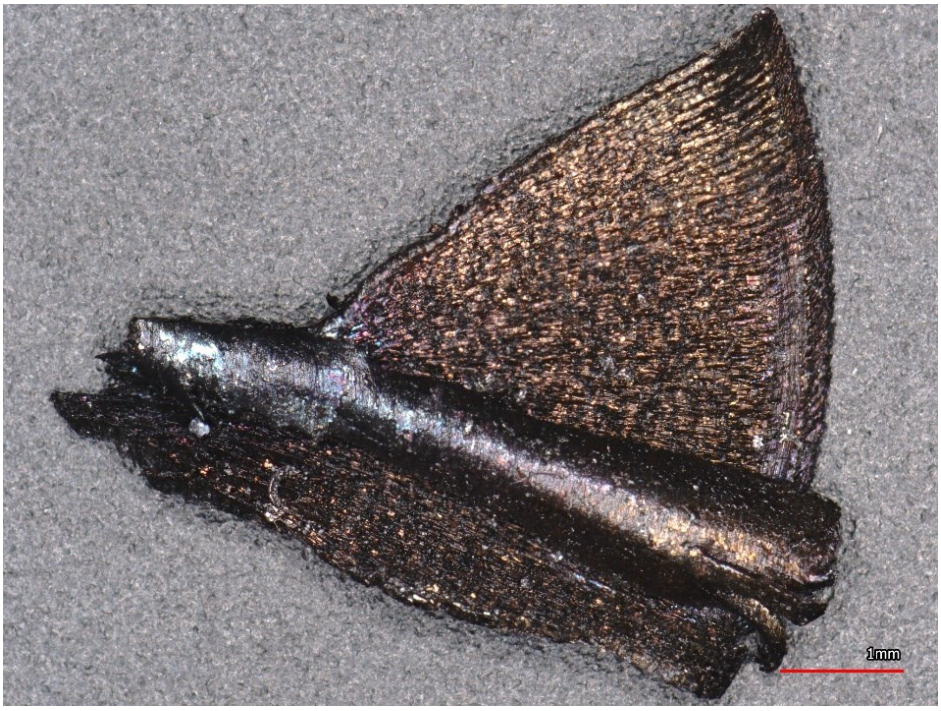

Figure 3.10: Typical short, segmented chip produced when drilling ADI.

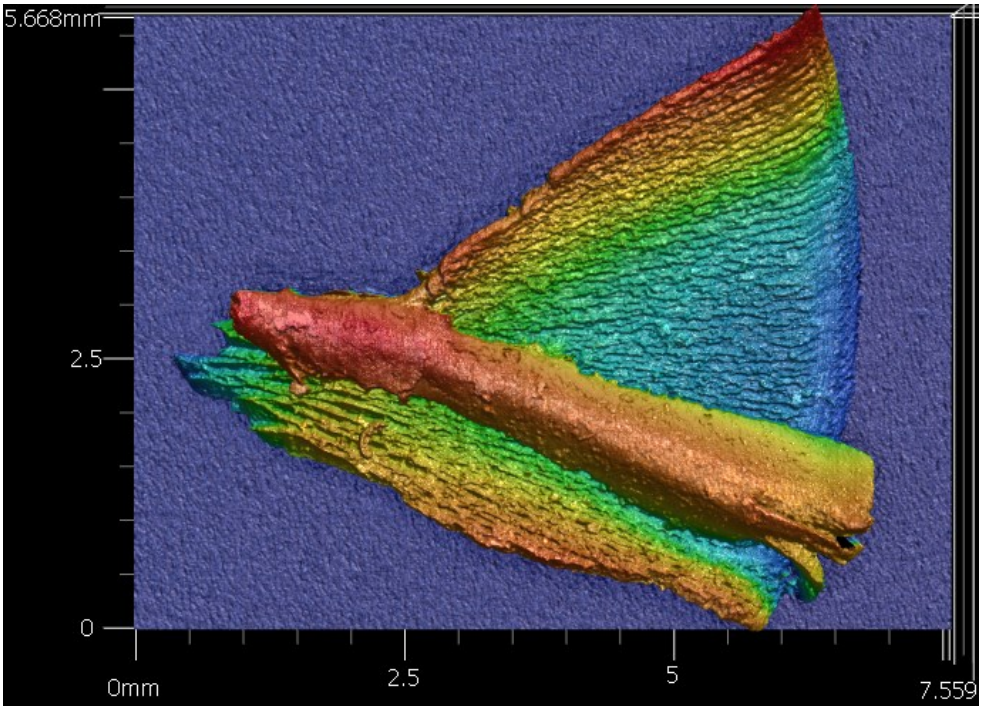

Figure 3.11: Topographical image of the short, segmented ADI chip.

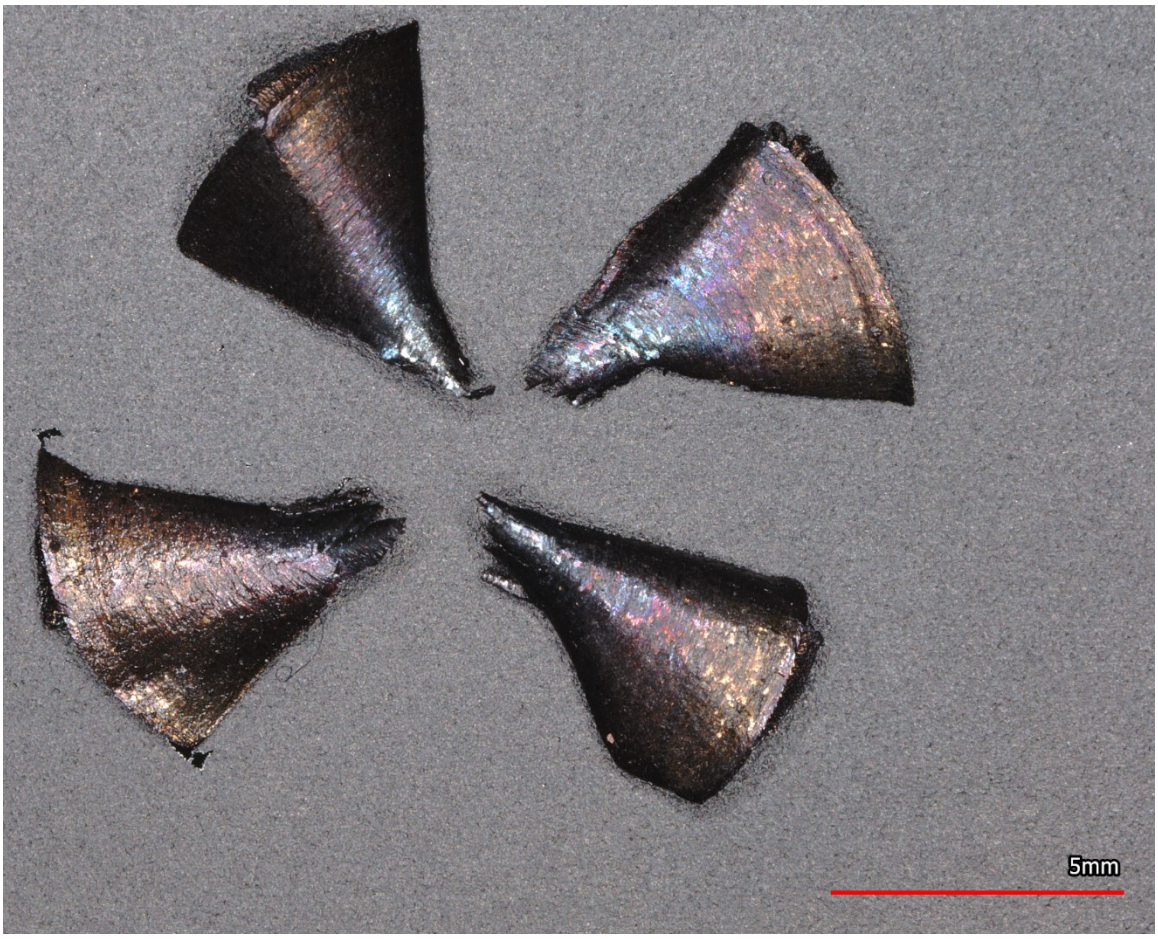

Figure 3.12: Segmented chips from drilling flipped. Coloring indicates chip carried heat away from the machining area. Also suggests that through spindle coolant may be necessary to properly cool and lubricate the tool when deep drilling and tapping.

Figure 3.13: Medium length continuous ADI chip from drilling. Note the serrations at the point.

Figure 3.14: Long continuous ADI drilling chip curling along a constantly tightening spiral.

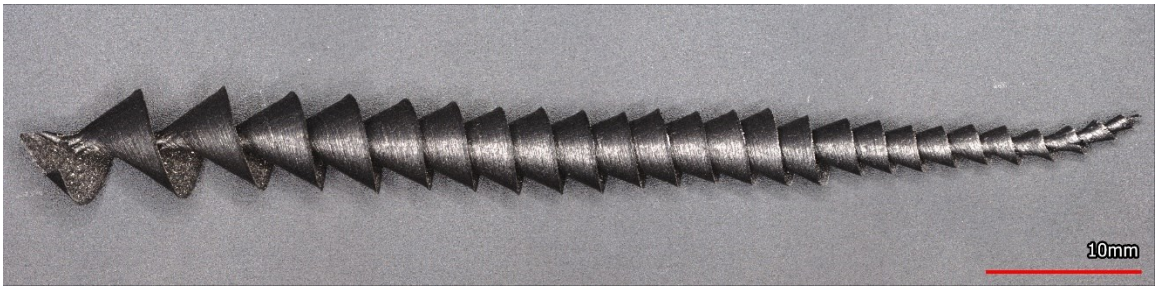

Figure 3.15: Long continuous chip from drilling as-cast 65-45-12 ductile iron.

3.1.6 Thread Profile and Surface Finish

As previously indicated, threads were machined to a class 2B fit. Class 2A fasteners successfully threaded into all holes produced in the study. Thread surface finishes were evaluated on the center hole of the 3-hole cross sections, this was hole number 13 in the order placed on the block. 3D height scans of the sample can be found in Figure A.9 through Figure A.16. Surface profilometry data of the threads was taken at 7 evenly spaced points along the major diameter for each sample as seen in Figure A.17. The results of the surface finish data collection can be found in Table 3.3 below.

Table 3.3: Sample Surface Finish

Sample	Drilled at Heat Treat	Threading Method	Measurement	Ra (µm)
1A	Predrilled	Form Tapped	Ave.	3.587
			Std. DV	0.589
2A	Predrilled	Cut Tapped	Ave.	4.168
			Std. DV	0.689
3A	Predrilled	Thread Milled	Ave.	2.868
			Std. DV	0.178
4A	Predrilled	Form Tapped	Ave.	3.046
			Std. DV	0.456
5A	Solid	Form Tapped	Ave.	5.028
			Std. DV	1.173
6A	Solid	Cut Tapped	Ave.	2.182
			Std. DV	0.288
7A	Solid	Thread Milled	Ave.	1.887
			Std. DV	0.282
8A	Solid	Form Tapped	Ave.	3.712
			Std. DV	1.070

3.1.7 Metallography After Machining

Threads from each specimen were cross sectioned, polished, etched, heat tinted, and documented on a light microscope. Variations in lighting conditions and automatic adjustments from the image processor resulted in different color saturation and exposure between samples. This makes any conclusions based solely on color comparison between

specimens misleading. The lighting and color balance issue is also present between different regions of the same sample. Comparison of machined regions to undisturbed areas provide the greatest insight on what changes took place within the microstructure. Typical microstructures observed at the machined surfaces created by the different threading operations can be seen in the images below in Figure 3.16 through Figure 3.18.

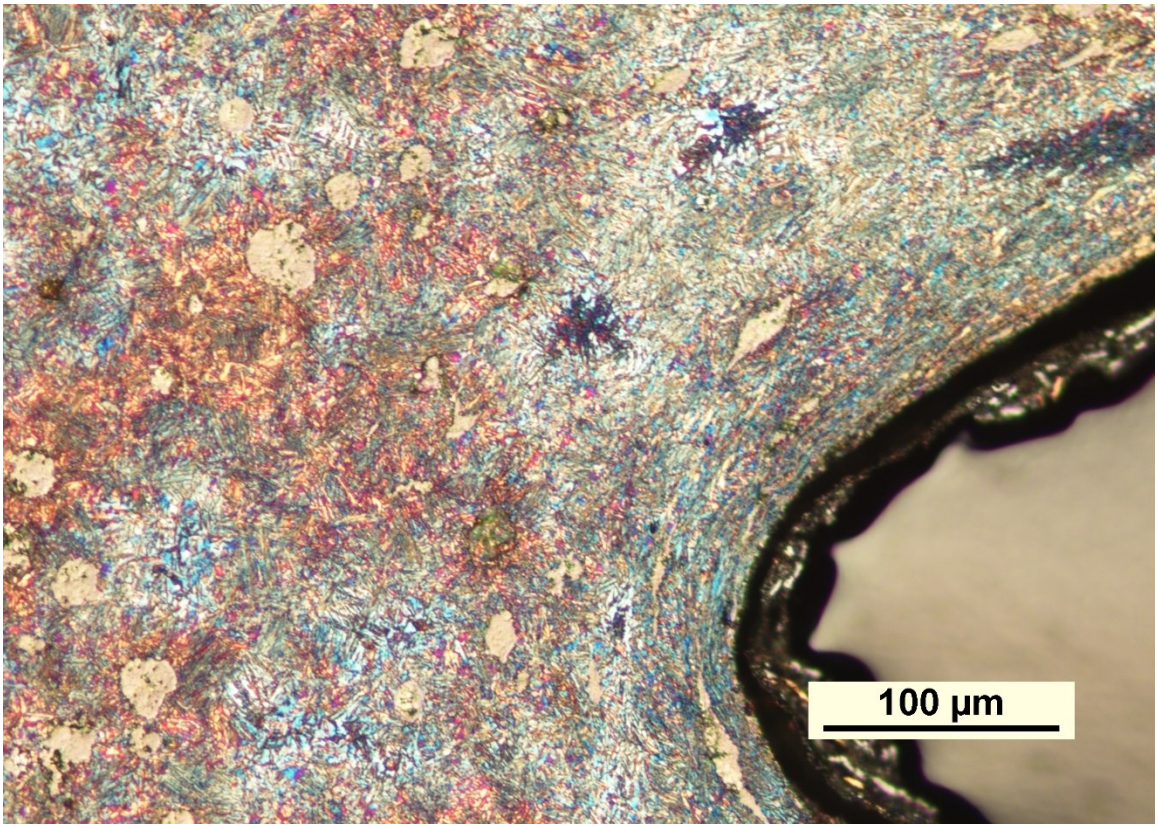

Figure 3.16: Sample 1A formed (50%) thread valley heat tinted microstructure.

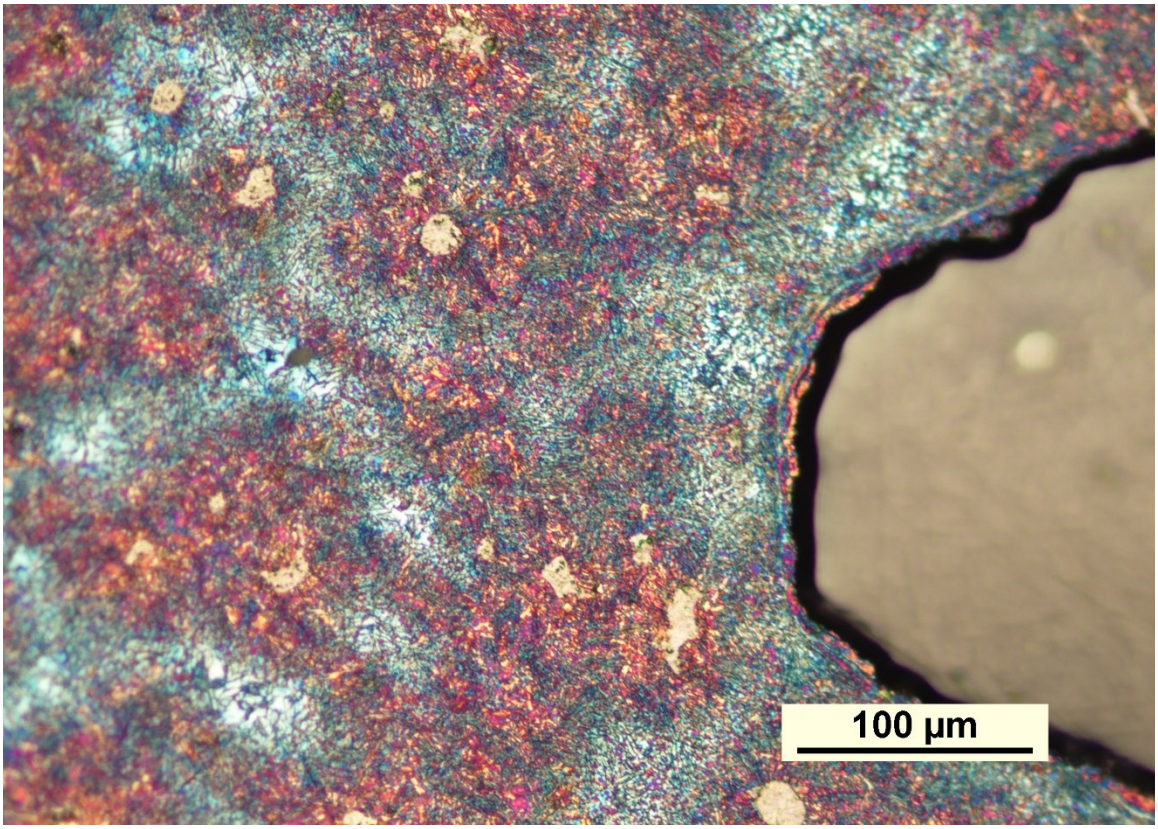

Figure 3.17: Sample 2A cut thread valley heat tinted microstructure.

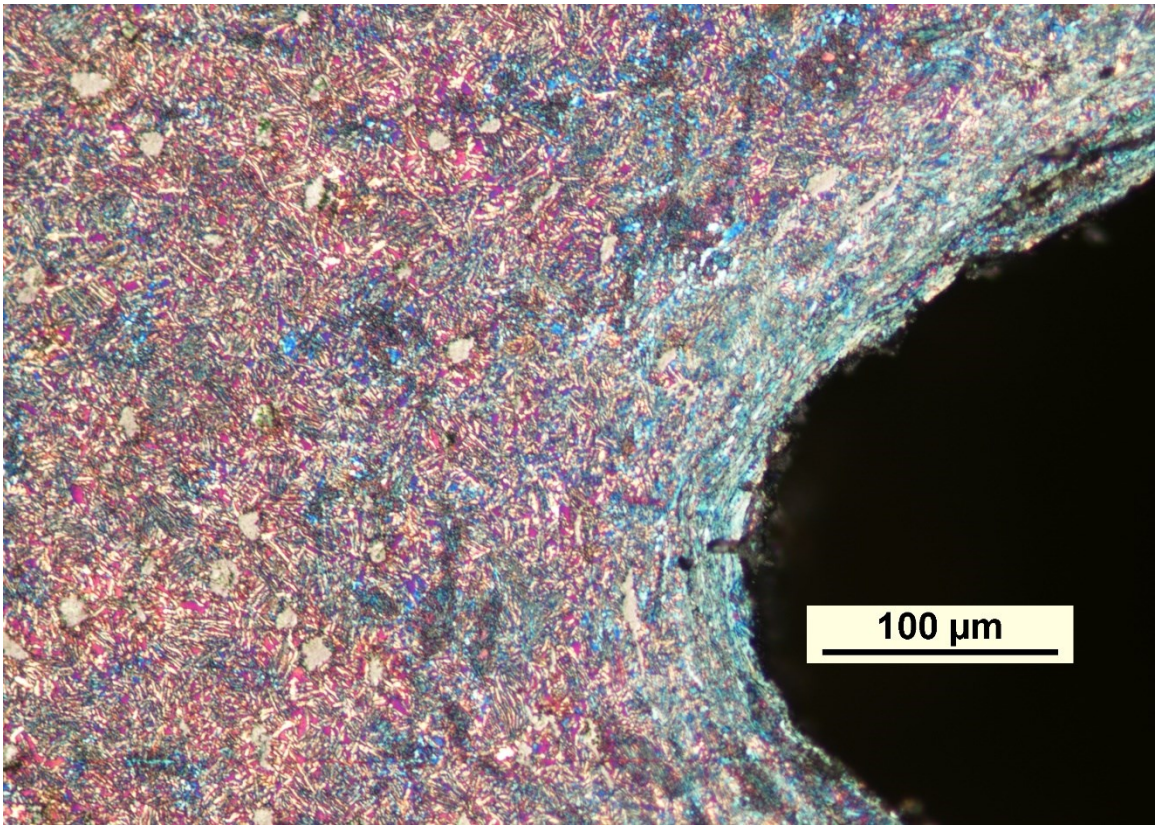

Figure 3.18: Sample 4B Formed (75%) thread valley heat tinted microstructure.

3.2 Discussion

When compared to a cut tapping operation, thread milling generates significantly less force because the work is drawn out over a greater amount of time. The parameters of the study yielded thread milling cycles that were 43 times longer than their cut tapping counterparts. While the productivity of tapping on the basis of time is far superior to thread milling there are certain advantages that a manufacturer may consider before writing off thread milling as an option. These include a reduced rigidity demand which can enable smaller, lower powered machines with inferior kinematic design to complete the operation when the same machine would not have the capability of threading the same component with a tap. Another consideration is that many milling machines are not

equipped with spindle synchronization on a standard build, and it is commonly an option that costs several thousands of dollars and cannot be retrofitted once the machine has left the factory. Without spindle synchronization, a CNC mill could only cut threads with a tap by using a clutched tapping head or specialized toolholders designed to float along the tool axis, but these setups are bulky, expensive, and reduce the machines available Z-axis travel. They are also typically incompatible with an automatic tool changer. For many existing machine shops equipped with older mills, thread milling may be the only viable option for threading ADI with the automation available on hand.

The threading operations that utilized synchronized tapping were quicker than the thread milling operation. There are several changes that could be used to improve thread milling cycle time. Feed rate could be increased, which would increase the feed per tooth, producing a larger chip and ultimately removing the required amount of material in fewer rotations of the spindle. If spindle speed is held constant this would reduce the amount of time required to finish the thread. Increasing spindle speed would increase the tool SFM, if FPT is held constant this would increase the feed rate proportionally which would also reduce the amount of time to complete the tool path. Radial engagement of the tool could be increased to the point that the number of stepovers is reduced which would have a dramatic impact on cycle time. Finally, a tool with a more sets of teeth along the desired thread pitch could be used to complete the thread while requiring the machine to perform fewer helical interpolations.

The rigid taps, both cut and forming, do not have the same level of adjustability as a thread mill. Material engagement on the teeth is determined by the size of the tap drill and feed rate is locked to spindle speed by the pitch of the thread. Threading parameters

that can be adjusted with a thread mill are SFM, FPT, and radial engagement. The most productive solution is likely to be the optimization of all parameters. It is likely that the cutter used in the study could be pushed to a more aggressive feed rate, and a faster spindle speed yielding a greater material removal rate and ultimately produce threads at a more competitive rate.

The parameters used in the study were recommended by a member of Harvey Tool's technical support team. It was explained that the parameters were derived from information presented in Handayani's [12] work in general milling of ADI rather than from a table of recommendations specific to the application in this study. This highlights the need of research regarding the ideal feeds and speeds for machining operations in ADI.

The results from the force analysis appear to suggest the samples drilled after austempering resist deformation in the subsequent threading operation more than samples that were drilled prior to austempering. Presumably this is due to the drilling operation imparting SIT on the material. The number of holes and specimens within the study were not sufficient to confidently claim that drilling after heat treating produces a hole that is more difficult to tap than a hole that is drilled then heat treated. However, it is an interesting observation that should be studied more in depth.

Comparison of the metallographic images of the heat tinted formed threads and cut threads appears to confirm the theory that SIT would occur to a higher degree in threads that were formed. The characteristic traits of a formed thread are present in ADI. The flow of the grain structure along the path of the thread is apparent, and the material curled to a point leaving a small channel at the thread crest.

Keough *et al.* [7] contend that roll forming threads is the most difficult machining operation to perform in ADI due to SIT. At the point that a machine can no longer drive the tool or hold the workpiece this is true. Using a cut tap in those situations would reduce the power and work holding demands. However, as long as a machine is not at its limits, thread forming produces high quality threads that could have superior mechanical properties when compared to cut threads. The tooling could also have an improved service life over cut taps, reducing tool changes and spindle downtime. While thread forming may not be suitable for all applications and may be limited to only the lowest grades of ADI, it is a viable option for threading grade 1 ADI and under the conditions of this study it performed very well.

4. CONCLUSIONS

The machinability of grade 1 ADI during cut tapping, form tapping, and thread milling operations was evaluated. Form tapping was found to be a viable method of threading grade 1 ADI. The SIT properties of ADI coupled with the abrasive wearing mechanism on tooling could incentivize a manufacturer to utilize form tapping over cut taps. Form tapping consumes more energy than alternative cutting operations, and as thread size grows, the limits of the machine and the setup will be met sooner when forming than when cutting.

Thread milling was much slower than the other two methods with the parameters utilized in this study. Threadmilling cycle times stand to gain the most improvement from optimization of machining parameters and tooling. Despite longer cycle times, thread milling boasts advantages over the rigid tapping operations in certain situations. In the event of catastrophic tool failure, the thread mill is much easier to recover from without scrapping the part. Additionally, cooling for thread milling is easier, and the requirements for spindle power and setup rigidity are much lower.

Cut tapping is a method that was known to work in ADI. It strikes a balance between tooling cost, cycle time, and thread quality. It is easy to see why cut tapping is the default threading method, and in many situations, it would be the most appropriate choice. Manufacturers should be aware of the alternative options at their disposal for situations where thread forming or thread milling might be a better option.

Drilling ADI components prior to austempering results in hole movement proportional to the part's size. Growth due to austempering could be anticipated and compensated for effectively with proper process control at the casting stage. For

applications without very tight tolerances this approach could reliably negate the need to machine heat treated iron.

4.1 Future Research

As stated earlier, for ADI to be embraced and incorporated into designs it needs to be more fully understood. This presents a number of recommendations for topics of future research listed below.

- A study to determine more optimal feed and speed recommendations for the three threading operations used in this paper.
- Preferred lubrication/cooling methods for drilling in ADI.
- A study to determine if drilling holes after heat treating results in holes that are more difficult to tap than holes that were drilled as-cast and then heat treated.
- A tool life study to evaluate the endurance capabilities of the three types of tools used in this study
- A class of fit study to evaluate the thread fit capabilities of the three methods and to compare the degradation of classes of fit as tools wear.

4.2 Post Experimental Thoughts

The material selected for the machinability experiments was a 65-45-12 ductile iron with a ferritic/pearlitic matrix. This material was selected because it was thought to have better heat treatability. It was later learned that when austempering, a higher grade ductile iron with a fully pearlitic matrix is more desirable as the lamellar iron-iron carbide structure most evenly distributes carbon throughout the matrix, this aids in carbon saturation of the austenite during austenitizing[3].

APPENDIX SECTION

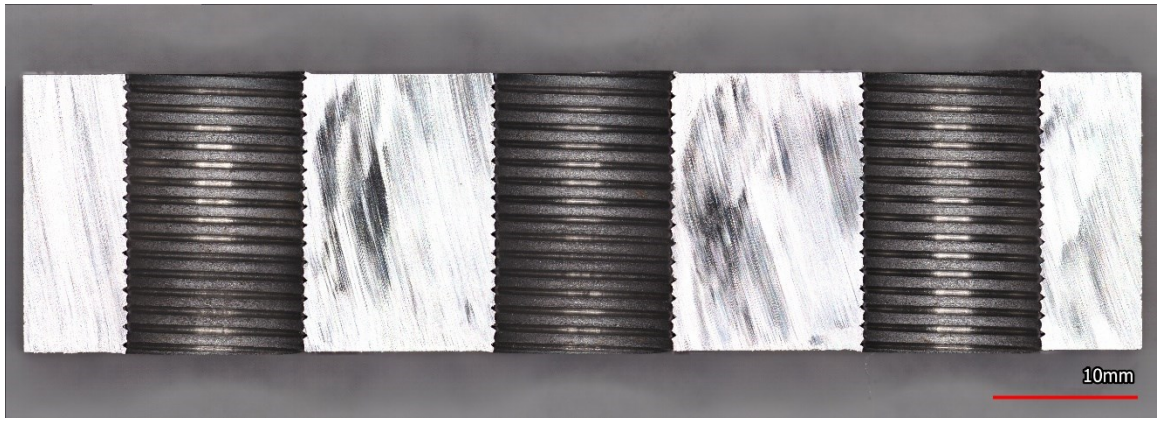

Figure A.1: Block 1A cross sectioned holes 1, 13, 7.

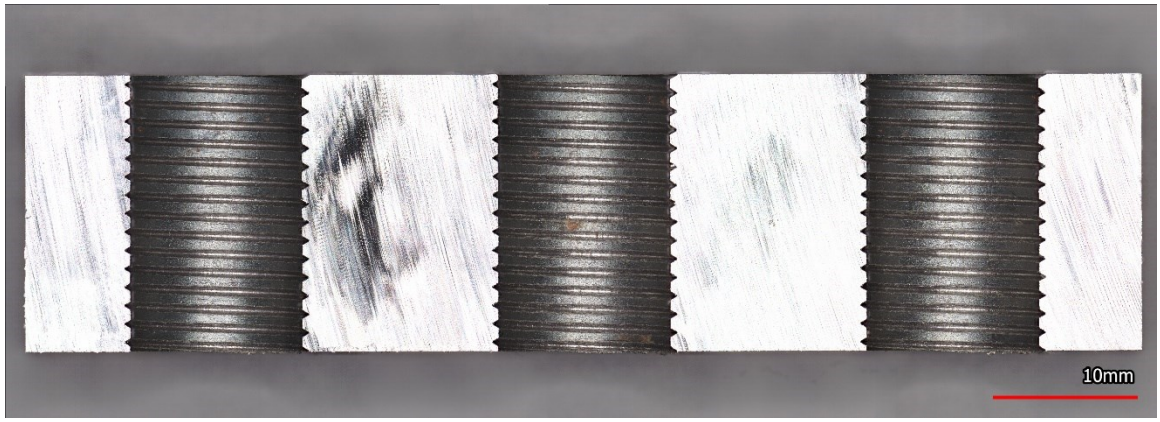

Figure A.2: Block 2A cross sectioned holes 1, 13, 7.

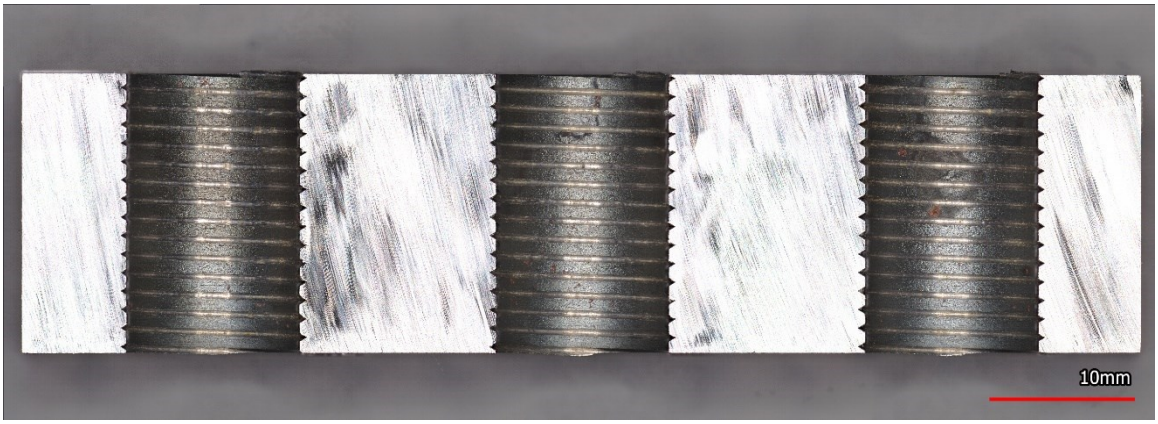

Figure A.3: Block 3A cross sectioned holes 1, 13, 7.

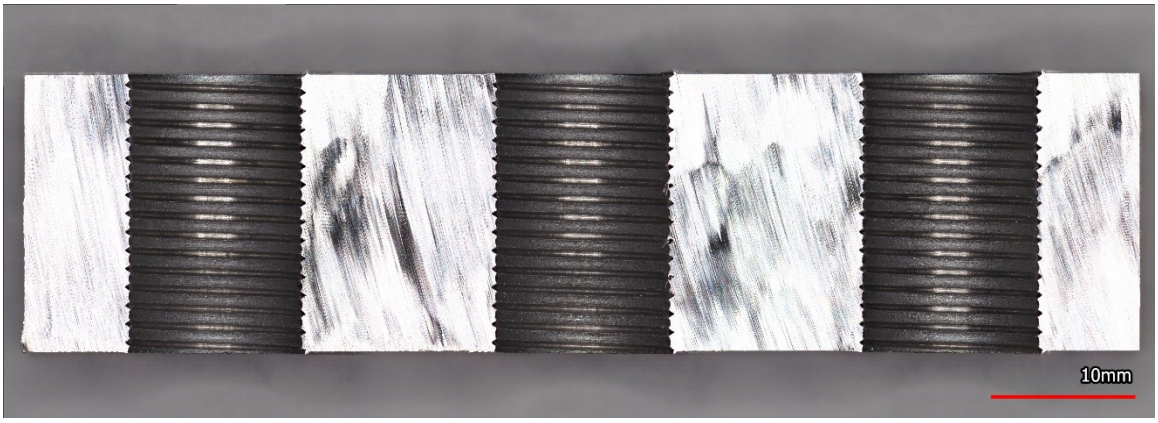

Figure A.4: Block 4A cross sectioned holes 1, 13, 7.

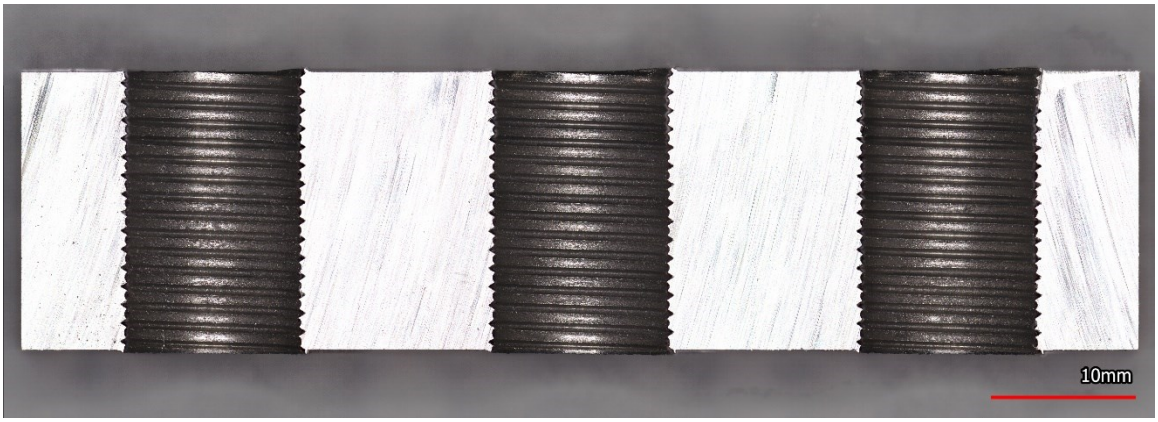

Figure A.5: Block 5A cross sectioned holes 1, 13, 7.

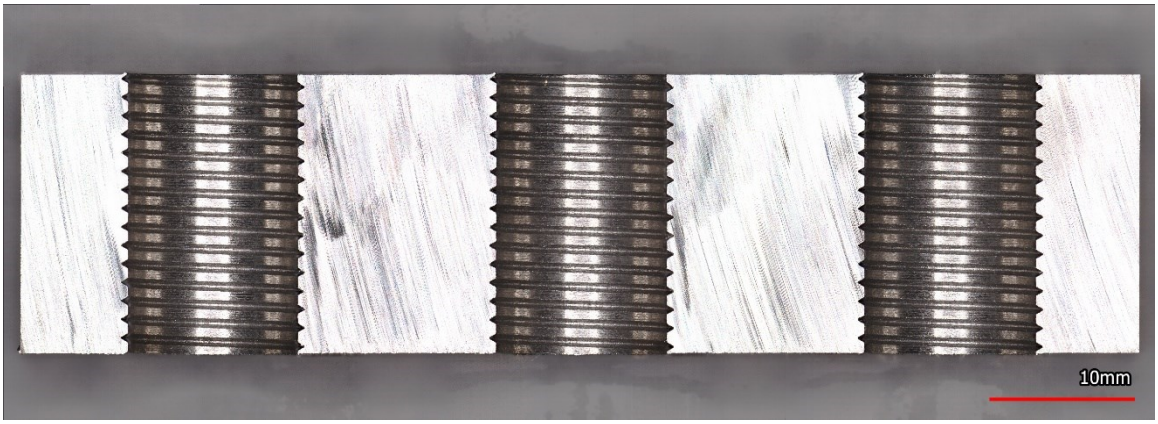

Figure A.6: Block 6A cross sectioned holes 1, 13, 7.

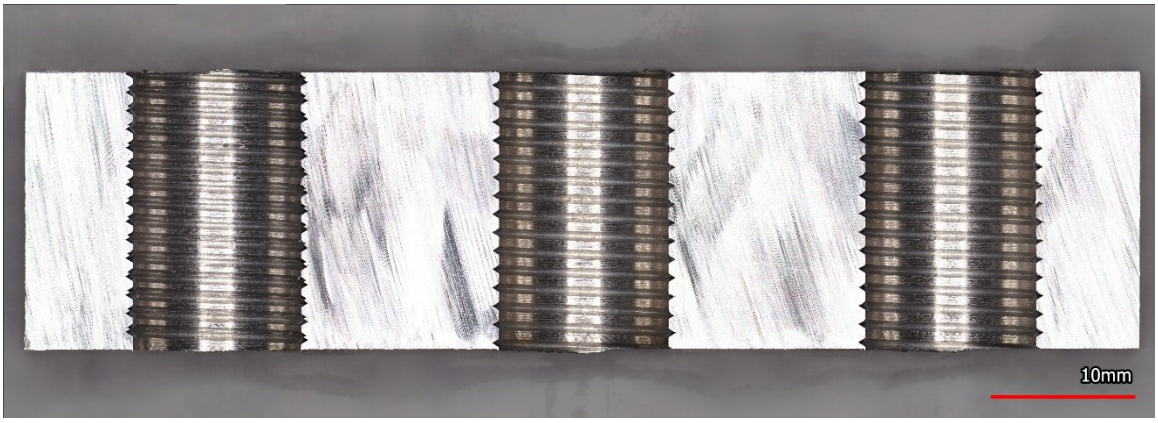

Figure A.7: Block 7A cross sectioned holes 1, 13, 7.

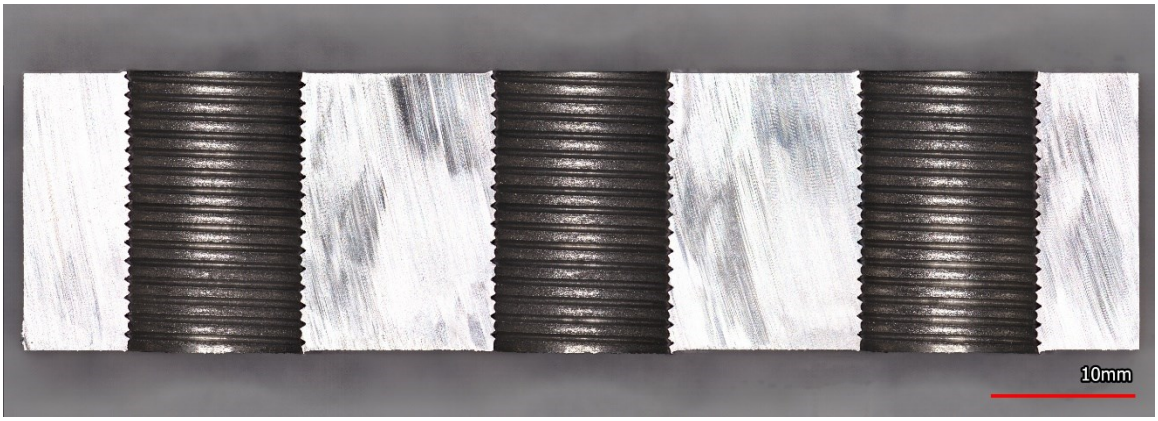

Figure A.8: Block 8A cross sectioned holes 1, 13, 7.

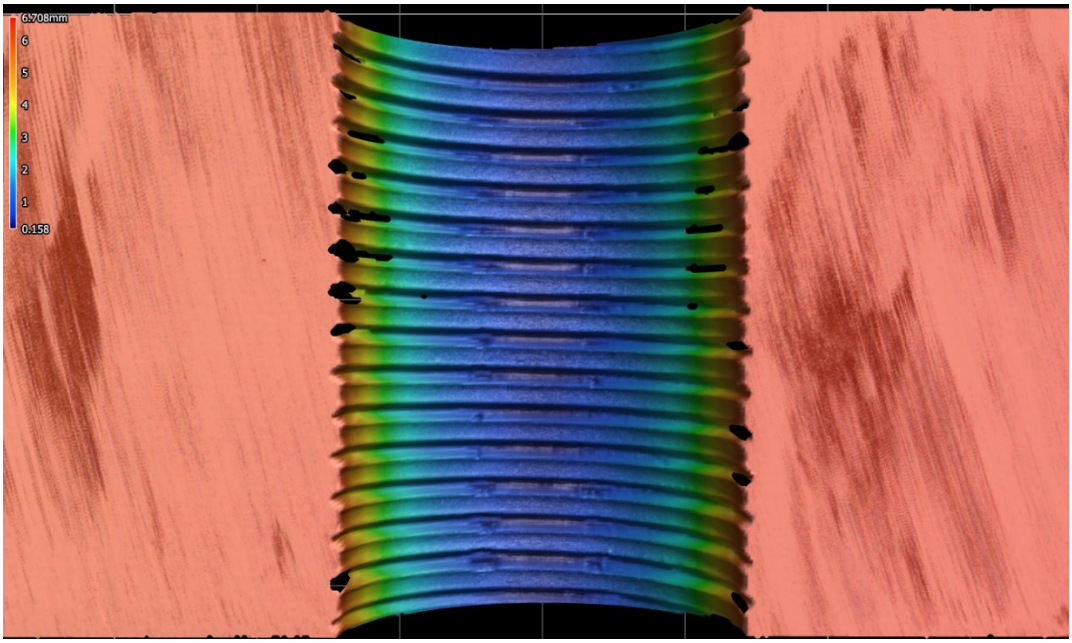

Figure A.9: Specimen 1A hole 13 cross section 3D scan.

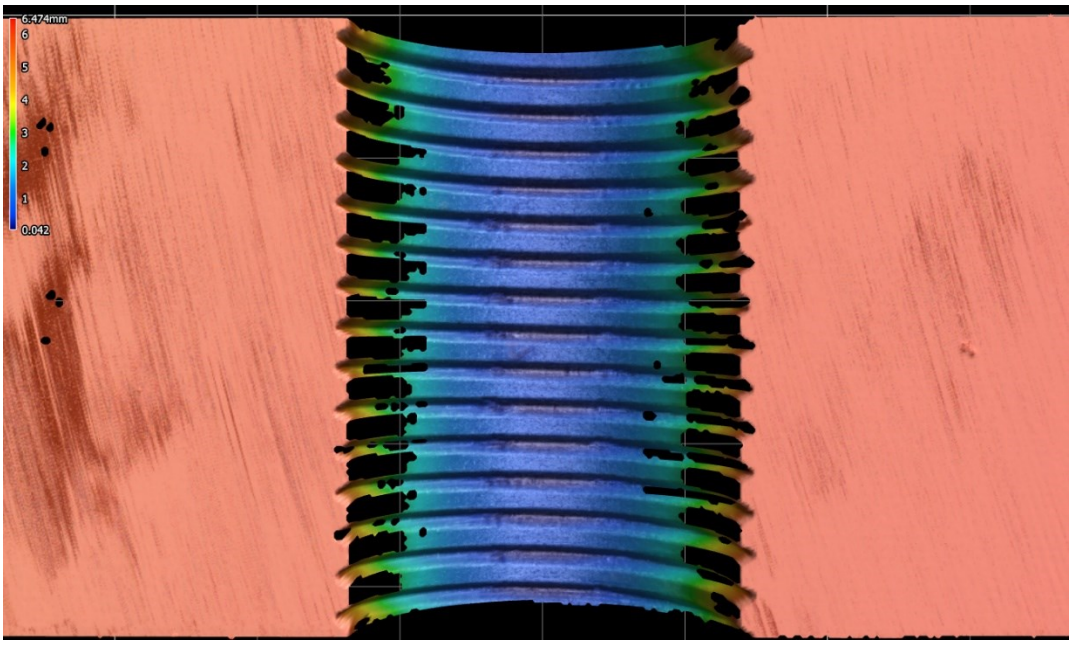

Figure A.10: Specimen 2A hole 13 cross section 3D scan.

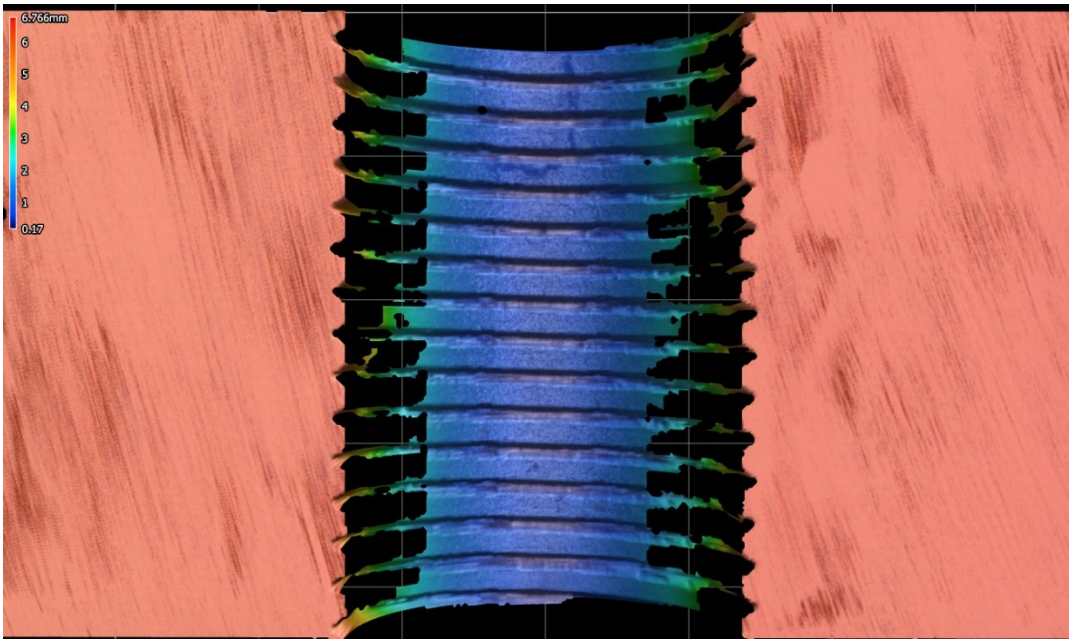

Figure A.11: Specimen 3A hole 13 cross section 3D scan.

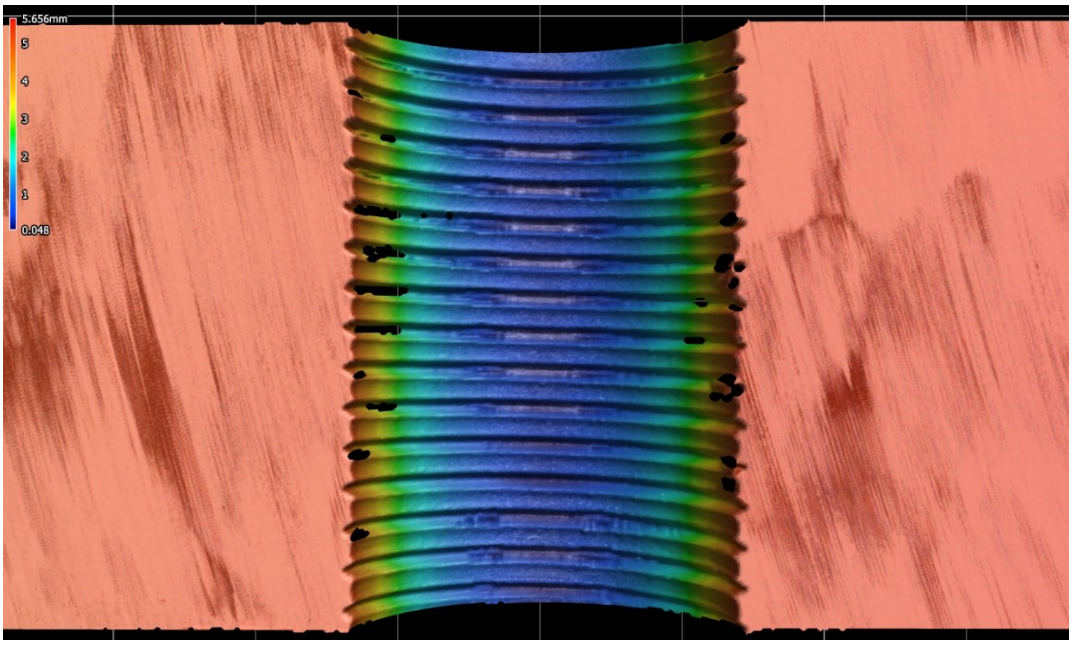

Figure A.12: Specimen 4A hole 13 cross section 3D scan.

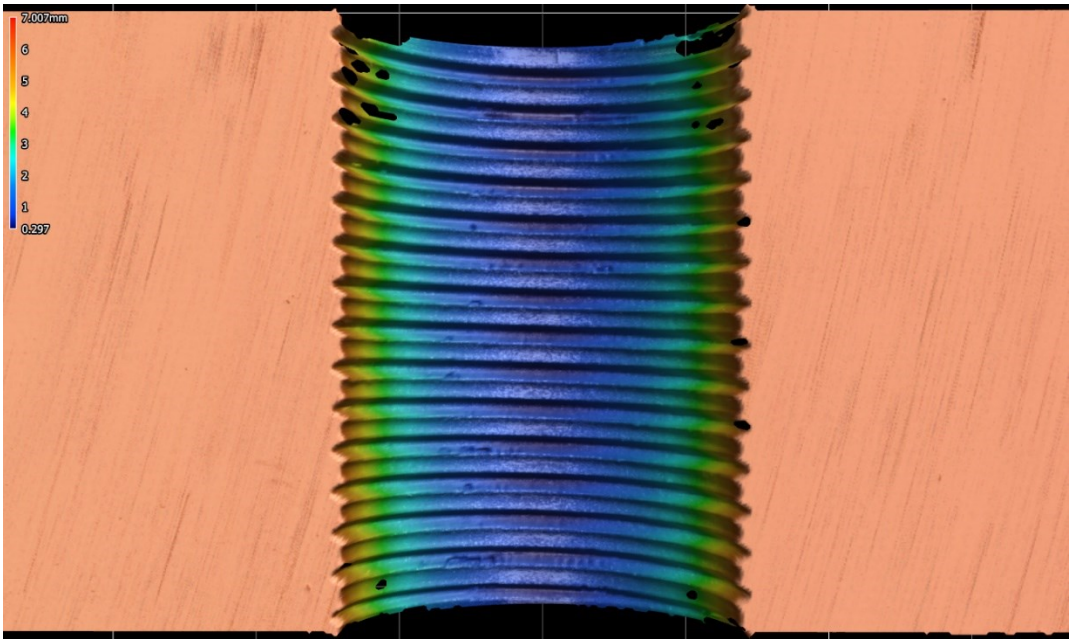

Figure A.13: Specimen 5A hole 13 cross section 3D scan.

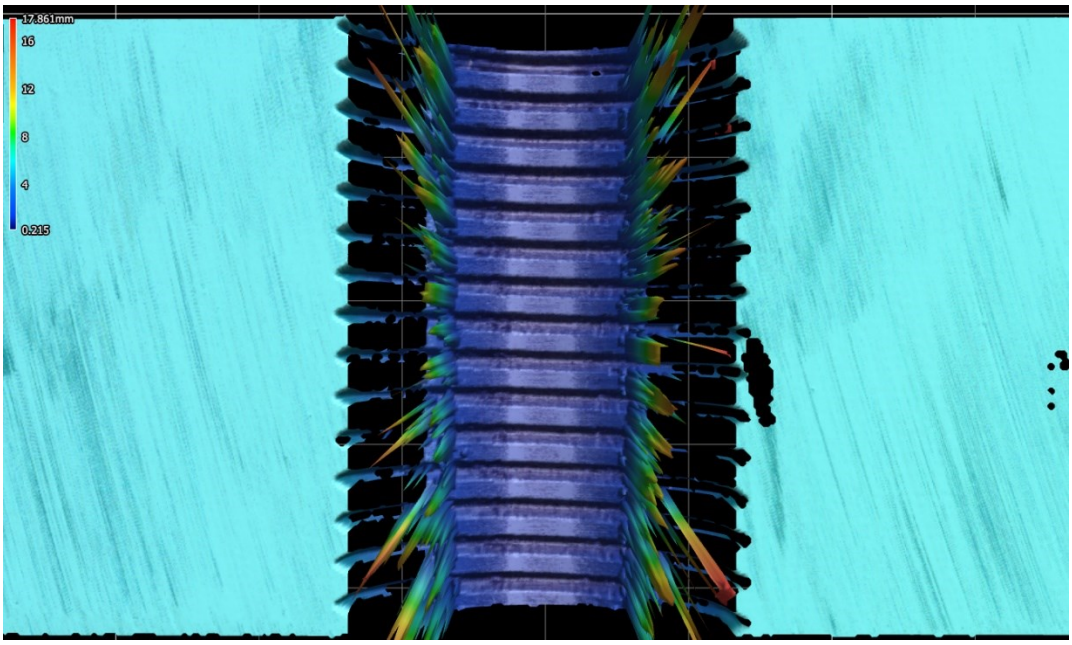

Figure A.14: Specimen 6A hole 13 cross section 3D scan.

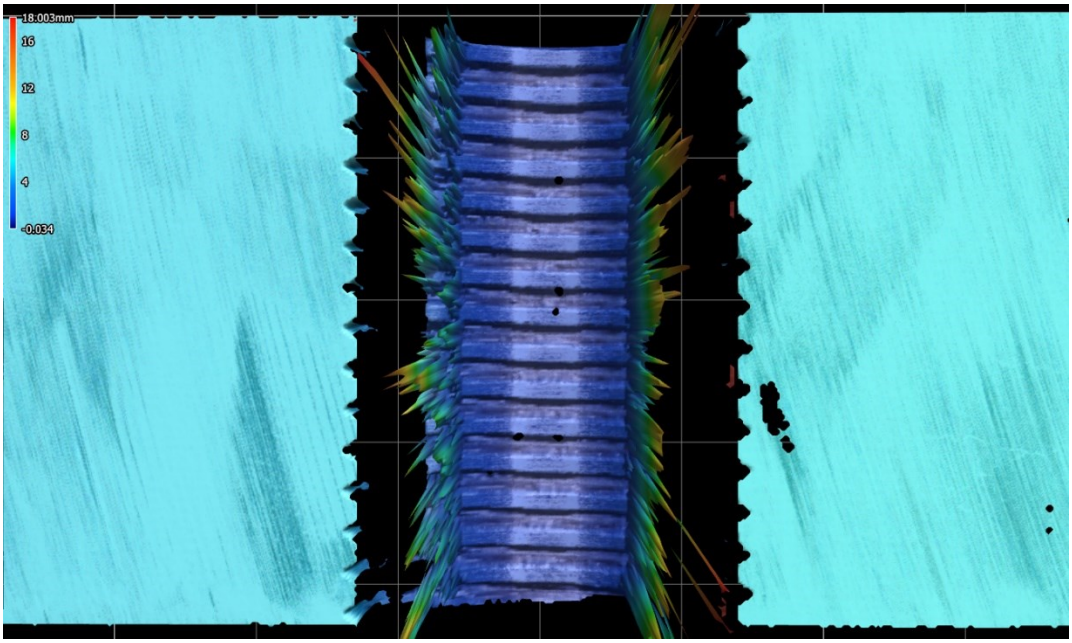

Figure A.15: Specimen 7A hole 13 cross section 3D scan.

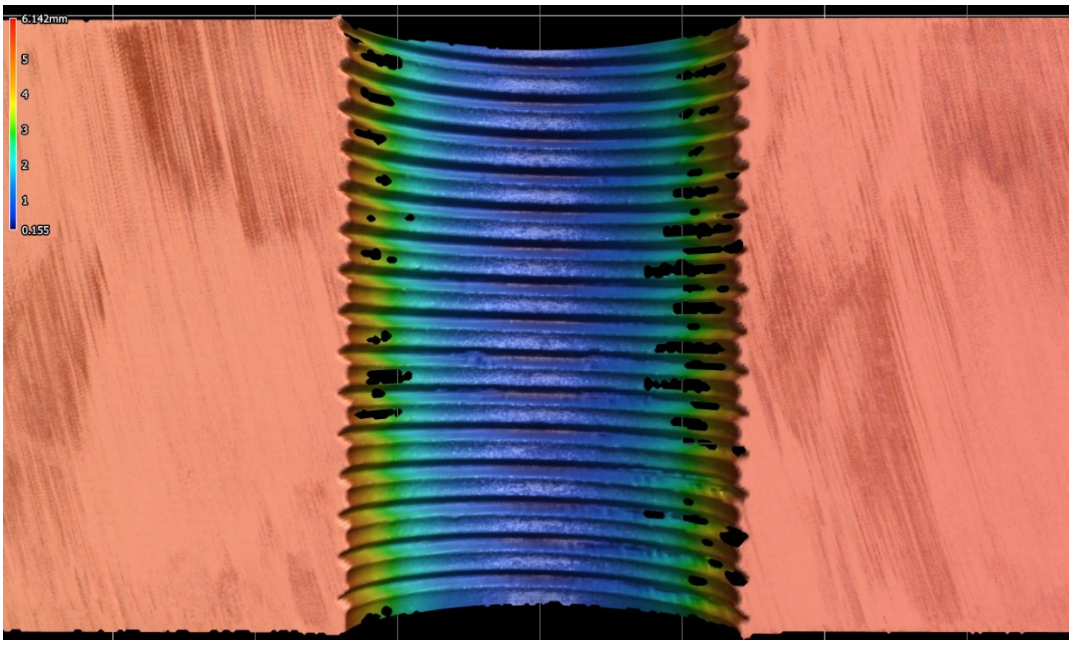

Figure A.16: Specimen 8A hole 13 cross section 3D scan.

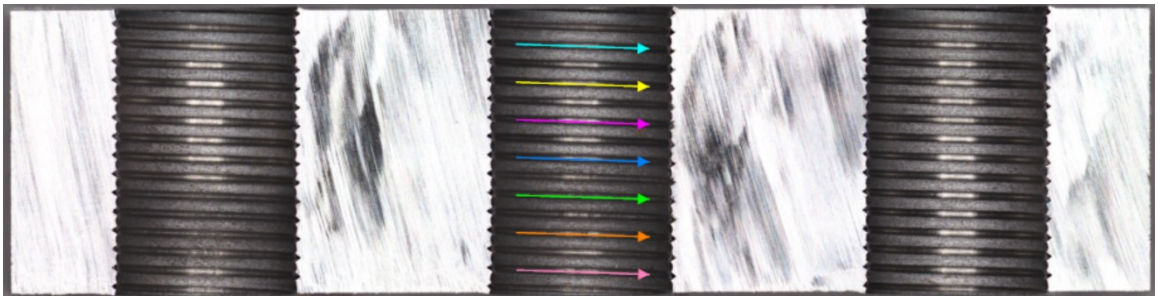

Figure A.17: Typical thread surface profilometry data points.

Table A.1: Iron Specimen Physical Dimension Growth after Austempering

Sample	**Change in Dimensions (in)**						
	1	2	3	4	L	W1	W2
1A	0.00040	0.00085	0.00060	0.00090	0.0050	0.0020	0.0030
2A	0.00050	0.00100	0.00065	0.00060	0.0050	0.0020	0.0025
3A	0.00100	0.00085	0.00040	0.00035	0.0055	0.0030	0.0025
4A	0.00035	0.00030	0.00085	0.00085	0.0060	0.0030	0.0025
5A	0.00095	0.00130	0.00120	0.00125	0.0045	0.0020	0.0015
6A	0.00070	0.00060	0.00075	0.00045	0.0050	0.0015	0.0020
7A	0.00070	0.00070	0.00070	0.00040	0.0045	0.0010	0.0020
8A	0.00075	0.00095	0.00070	0.00065	0.0045	0.0005	0.0020
4B	0.00050	0.00065	0.00065	0.00085	0.0040	0.0020	0.0020

REFERENCES

[1] J. R. Keough and K. L. Hayrynen, "Automotive Applications of Austempered Ductile Iron (ADI): A Critical Review," *SAE Trans.*, vol. 109, pp. 344–354, 2000.

[2] S. Samaddar, T. Das, A. K. Chowdhury, and M. Singh, "Manufacturing of Engineering components with Austempered Ductile Iron – A Review," *Mater. Today Proc.*, vol. 5, no. 11, pp. 25615–25624, 2018, doi: 10.1016/j.matpr.2018.11.001.

[3] B. Kovacs, "Austempered Ductile Iron Fact and Fiction." 1990.

[4] F. C. (Flake C.) Campbell 1946-2012, ed., *Elements of metallurgy and engineering alloys*. ASM International, 2008. [Online]. Available: https://libproxy.txstate.edu/login?url=https://search.ebscohost.com/login.aspx?direct=true&db=brd&AN=116293539&site=eds-live&scope=site

[5] E. Oberg, F. D. Jones, H. L. Horton, H. H. Ryffel, and C. J. McCauley, *Machinery's Handbook: A Reference Book for the Manufacturing and Mechanical Engineer, Designer, Drafter, Metalworker, Toolmaker, Machinist, Hobbyist, Educator, and Student*. Industrial Press, Incorporated, 2020. [Online]. Available: https://books.google.com/books?id=VN5EzQEACAAJ

[6] K. L. Hayrynen, "The Production of Austempered Ductile Iron (ADI)," presented at the World Conference on ADI, 2002.

[7] J. R. Keough, K. L. Hayrynen, and V. M. Popovski, "Continuing Developments in the Science and Application of Austempered Ductile Iron (ADI)," p. 10.

[8] "Four Distinctions Between Tungsten Carbide And HSS | XYMJ," *Zigong Xingyu Cemented Carbide Dies&Tools Co.,Ltd*. https://www.xymjcarbide.com/articles/detail/four-distinctions-between-tungsten-carbide-and-hss.html (accessed Oct. 20, 2022).

[9] "Chuck the chips." https://www.ctemag.com/news/articles/chuck-chips (accessed Jun. 14, 2021).

[10] M. Wan and Y. Altintas, "Mechanics and dynamics of thread milling process," *Int. J. Mach. Tools Manuf.*, vol. 87, pp. 16–26, Dec. 2014, doi: 10.1016/j.ijmachtools.2014.07.006.

[11] G. M. Goodrich American Foundry Society. ,. Cast Iron Division. ,. A5 Committee. ,., *Iron castings engineering handbook*. Des Plaines, Ill.: American Foundry Society, 2004.

[12] D. Handayani, “The Machinability of Austempered Ductile Irons (ADI),” Ph.D., The Pennsylvania State University, United States -- Pennsylvania, 2017. Accessed: Jan. 27, 2020. [Online]. Available: http://search.proquest.com/pqdtglobal/docview/2021980123/abstract/7D43E7AE62C248D0PQ/1

[13] L. Larumbe, E. Delgado, M. Alvarez-Vera, and P. Villanueva, “Forming process using austempered ductile iron (ADI) in an automotive Pitman arm,” *Int. J. Adv. Manuf. Technol.*, vol. 91, no. 1–4, pp. 569–575, Jul. 2017, doi: 10.1007/s00170-016-9771-1.

[14] “Threads Will Roll.” https://www.ctemag.com/news/articles/threads-will-roll (accessed Oct. 20, 2022).

[15] I. Elosegui, U. Alonso, and L. Lopez de Lacalle, “PVD coatings for thread tapping of austempered ductile iron,” *Int. J. Adv. Manuf. Technol.*, vol. 91, no. 5–8, pp. 2663–2672, Jul. 2017, doi: 10.1007/s00170-016-9963-8.

[16] S. N. Sakharkar and R. S. Pawade, “Effect of Machining Environment on Turning Performance of Austempered Ductile Iron,” *CIRP J. Manuf. Sci. Technol.*, vol. 22, pp. 49–65, Aug. 2018, doi: 10.1016/j.cirpj.2018.04.006.

[17] G. Benga and I. Ciupitu, “The influence of coating and tool geometry on the tool life in a thread cutting process,” *Ann. DAAAM Amp Proc.*, pp. 91–93, Jan. 2008.

[18] H. M. Gewindeformer, “HPF Max – High Performance Forming HPF Max – High Performance Forming,” no. 6095, p. 12.

[19] J. L. Garin and R. L. Mannheim, “Strain-induced martensite in ADI alloys,” *J. Mater. Process. Technol.*, p. 5, 2003.